Validation of digestion and element separation methods and a new data reduction program (IsotopeHf®) for Lu-Hf isotope dilution analysis by MC-ICP-MS

Reneé González-Guzmán[1,*], Bodo Weber[1], María D. Tazzo-Rangel[1], and Luigi Solari[2]

[1] *División de Ciencias de la Tierra, Centro de Investigación Científica y de Educación Superior de Ensenada, Baja California, Carretera Ensenada-Tijuana 3918, Zona Playitas, 22860 Ensenada, Baja California, Mexico.*
[2] *Centro de Geociencias, Universidad Nacional Autónoma de México, Blvd. Juriquilla 3001, 76230 Juriquilla, Querétaro, Mexico.*
**rguzman@cicese.edu.mx*

ABSTRACT

The Lu-Hf isotope system is not only an important geochronometer but also a powerful tool for petrogenetic studies. To determine reliable analytical results of this system from rock and mineral samples, a protocol is established that includes appropriate sample digestion, a three-stage HREE-Hf ion-exchange separation procedure, a data acquisition protocol by MC-ICP-MS, and an R-based data reduction software package (IsotopeHf®) that transforms raw mass spectrometry data into meaningful isotopic ratios, including all the necessary corrections for spiked samples. Our $^{176}Hf/^{177}Hf$ results of both mafic and felsic geochemical reference standards agree with those reported by other authors. However, results obtained using PicoTrace® pressure digestion system (DAS®) yield significantly higher $^{176}Lu/^{177}Hf$ for felsic rocks with high Hf content (> 15 ppm) compared to data obtained by Parr® bomb dissolution, indicating incomplete digestion of HFSE-rich phases like zircon under specific conditions of DAS® digestion. The high degree of Hf purity attained using our chemical procedure, MC-ICP-MS measurement protocol, and the IsotopeHf® program yielded accurate data with reliable and reproducible Lu-Hf isotope ratios within typical analytical uncertainties.

Key words: Lu-Hf; MC-ICP-MS analysis; digestion methods; data reduction software; geochemical reference standards.

RESUMEN

El sistema isotópico Lu-Hf no es sólo un geocronómetro importante, también es una poderosa herramienta para estudios petrogenéticos. Para determinar resultados analíticos confiables de este sistema a partir de muestras de rocas y minerales, se establece un protocolo que incluye una adecuada digestión de la muestra, un procedimiento de separación HREE-Hf por cromatografia de intercambio iónico en tres etapas, un esquema para adquisición de datos por MC-ICP-MS y un software para la reducción de datos implementado en R (IsotopeHf®), en el que se incluyen todas las correcciones necesarias para muestras con trazador, convirtiendo el conjunto de datos de la espectrometría de masas en relaciones isotópicas significativas. Nuestros resultados en $^{176}Hf/^{177}Hf$ de los estándares de referencia geoquímica, tanto máficos como félsicos, son concordantes con aquellos reportados previamente por otros autores. Sin embargo, la comparación del sistema de digestión a presión (DAS®) de Picotrace® produce valores $^{176}Lu/^{177}Hf$ significativamente mayores en rocas félsicas con alta concentración de Hf (> 15 ppm) comparados con los obtenidos mediante bombas Parr®, indicando digestión incompleta bajo las condiciones específicas en la digestión DAS® para fases ricas en HFSE, como el zircón. La alta purificación de Hf en el procesamiento químico, el protocolo para las mediciones por MC-ICP-MS *y el programa IsotopeHf® producen datos exactos con relaciones isotópicas Lu-Hf confiables y reproducibles dentro de las incertidumbres analíticas típicas.*

Palabras clave: Lu-Hf; MC-ICP-MS análisis; métodos de digestión; software para reducción de datos; estándares de referencia geoquímica.

INTRODUCTION

Besides being a powerful geochronometer for garnet-bearing metamorphic rocks, especially eclogites (*e.g.*, Skora *et al.*, 2006; Smit *et al.*, 2010; Estrada-Carmona *et al.*, 2015) and phosphates (*e.g.,* Barfod *et al.*, 2003; Larsson and Söderlund *et al.*, 2005), the geological application of the Lu-Hf isotope system (β^-decay of ^{176}Lu to ^{176}Hf, $t_{1/2}$ = 37.2 Ga; Scherer *et al.*, 2001; Söderlund *et al.*, 2004) is mainly focused on the chemical differentiation of the silicate Earth with respect to the formation of crust and mantle (*e.g.*, Vervoort *et al.*, 2000; Blichert-Toft and Puchtel, 2010; Guitreau *et al.*, 2013), crustal contamination of mantle sources (*e.g.,* Cai *et al.*, 2014; Guo *et al.*, 2016), and sedimentary environments (*e.g.*, Bayon *et al.*, 2009; Vervoort *et al.*, 2011). In addition, when taken in combination with another isotopic system like Sm-Nd, mixing models can be calculated and deviations from the terrestrial trend can be identified (*e.g.*, Schmitz *et al.*, 2004; Vervoort *et al.*, 2011).

The first approaches to measure Lu-Hf isotope ratios in geological materials were made with Thermal Ionization Mass Spectrometry (TIMS, *e.g.*, Patchett and Tatsumoto, 1980). After the development

González-Guzmán, R., Weber, B., Tazzo-Rangel, M.D., Solari, L., 2016, Validation of digestion and element separation methods and a new data reduction program (IsotopeHf®) for Lu-Hf isotope dilution analysis by MC-ICP-MS: Revista Mexicana de Ciencias Geológicas, v. 33, núm. 2, p. 254-269.

of Multi-Collector Inductively Coupled Plasma Mass-Spectrometry (MC-ICP-MS) instruments in the early nineties, having a much greater ionization efficiency, as well as improvements in the chemical separation that diminished the isobaric interferences and matrix effects of other major and trace elements (Blichert-Toft *et al*., 1997; Blichert-Toft, 2001; Le Fèvre and Pin, 2001, 2005; Münker *et al*., 2001; Bizzarro *et al*., 2003; Ulfbeck *et al*., 2003; Lapen *et al*., 2004; Connelly *et al*., 2006; Lu *et al*., 2007; Sprung *et al*., 2010; Yang *et al*., 2010; Bast *et al*., 2015), the Lu–Hf isotope system became more popular both for applications in geochronology and in isotope geochemistry. In this context, the Lu-Hf separation method for whole-rock samples developed by Münker *et al*. (2001) is a benchmark procedure that is now emulated by many other laboratories (*e.g*., Bast *et al*., 2015). Recently, Sprung *et al*. (2010) improved this separation method performing additional Lu and Hf clean-up steps. This separation procedure facilitates additional separation of elements for other isotope systems like Rb-Sr and Sm-Nd from the same sample aliquot.

However, the contrasting chemical behavior of Lu and Hf, the content of refractory minerals (like garnet, zircon or rutile) in some igneous and metamorphic rocks, and the behavior of Hf from the spike, hampers the complete sample digestion and sample-spike equilibration. These complications may lead to systematic errors of up to ten εHf-units, especially in zircon-bearing rocks and even more when recalculated to an initial value in relatively old (pre-Mesozoic) rocks (Mahlen *et al.*, 2008). Problems with incomplete sample digestion by standard bench-top digestion methods were identified by various authors (Blichert-Toft *et al*., 1997; Münker *et al*., 2001; Ulfbeck *et al*., 2003; Blichert-Toft *et al*., 2004; Lapen *et al*., 2004; Mahlen *et al*., 2008; Vervoort *et al*., 2011) and were dealt by employing acid pressure digestion vessels (Parr® bombs) that consist of a steel jacket with a Teflon® liner. To ensure complete digestion in Parr® pressure vessels, the samples have to be digested typically for 5 days at ~190°C. However, a separate bomb is required either for every individual sample or two samples in Savillex® beakers can be put together in a larger Parr® bomb.

With the Picotrace® pressure digestion system (DAS®) 16 (or 32) samples can be digested simultaneously. The system consists of one (or two) Teflon-coated pressure block(s) made of metal alloy that hosts 16 Teflon pressure vessels, a Teflon-coated hot plate, and a hot plate controller. Besides that, the system is equipped with an evaporation device, with which strong acids such as perchloric and hydrofluoric acid are evaporated and neutralized in a closed system with no need of a perchloric acid fume hood. However, since the digestion block is heated on a hot plate and not in an oven, the active internal temperature is limited to ~165°C, due to loss of heat between the Teflon-coated hot plate, which is limited to a maximum temperature of 240°C and operated generally at 215°C, and the Teflon-coated digestion block that is located in a laminar flow clean-bench.

In this contribution we report (1) the chemical separation method established in the cleanlab facilities at the Geology Department, Centro de Investigación Científica y de Educación Superior de Ensenada (CICESE), México; (2) the analytical protocol employed for the Thermo Neptune MC-ICP-MS installed at Centro de Geociencias, UNAM, Juriquilla, Querétaro, México; (3) the equations used to correct the measured lutetium and hafnium mass intensities for isobaric interferences, instrumental mass-bias, and spike, which form the basis for the data reduction software written and developed in R language (R Core Team, 2016) and presented here (IsotopeHf®). External reproducibility and accuracy of the methods is validated by analyses of several international reference standards and replicate analyses of unknown samples. In addition, to evaluate the digestion efficiency of the Picotrace DAS® pressure digestion system some samples were digested in both the Parr® Acid Digestion Vessel and the Picotrace DAS®.

ANALYTICAL METHODS

Sample descriptions

Eight different international reference rock powders recommended by the United States Geological Survey (USGS, n=6) and the Geological Survey of Japan (GSJ, n=2) were analyzed, as well as six replicate digestions of unknown whole-rock samples. The unknown samples are from the Chiapas Massif, Southern México, and they were selected on the basis of their mineralogical composition and age: Two felsic orthogneiss samples (age ~1.0 Ga) and one garnet-bearing sillimanite schist (age ~0.45 Ga) were chosen by containing significant amounts of resistant phases such as zircon or garnet, and three zircon-poor mafic amphibolite samples (age ~0.45 Ga) were analyzed to further examine the accuracy and precision of our method. Additionally, five single zircon grains and four fractions of amphibole concentrates were analyzed. A brief description of the samples is provided in Table 1.

Chemical procedures

Chemical preparation and element separation were performed in PicoTrace® clean benches within class 1000 cleanlab facilities at the Geology Department, CICESE. All acids used were double distilled in subboiling Teflon® systems, and all Teflon® beakers were previously cleaned in aqua regia, HNO_3, HF, and Milli-Q® water. Between 50–150 mg of powdered whole rock aliquot or amphibole concentrate was weighted (to 0.01 mg precision) into a digestion vessel and spiked with a mixed ^{180}Hf–^{176}Lu tracer (MS-WR-1, ^{180}Hf=98.266% and ^{176}Lu=71.610%) provided by the Institut für Mineralogie, Universität Münster, Germany. When the Picotrace DAS® was used, a mixture of concentrated HF, HNO_3, and $HClO_4$ (3–4 mL, ~1 mL and 3–4 drops, respectively) was added to each sample and placed on a hot plate at 215 °C for one week. When the Parr® Acid Digestion Vessel was used for digestion, a mixture of HF–HNO_3 (5:1) was added to the samples previously weighted into 7 ml Savillex® beakers. Two Savillex® beakers were placed into the Teflon liner of a 125 ml Parr® Acid Digestion Vessel together with concentrated HF as a pressure medium and heated at 190 °C for five days in an oven.

Evaporation of acids at subboiling conditions (including $HClO_4$) was performed with the Picotrace DAS® (for both DAS® and Parr® digested samples), changing the system to evaporation assembly and using hotplate temperatures starting at 120 °C (~75 °C evaporation temperature for HF and HNO_3) and a stepwise heating program that goes up to 160 °C (~120 °C evaporation temperature) to dry down the perchloric acid. Strong acid fumes are extracted from the DAS® with a clean air current in a closed system and neutralized by passing them through wash-bottles filled with 5% NaOH solution. The resulting perchlorates were converted into chlorides by adding ~5 mL of 6M HCl. Sample-spike equilibration was achieved by leaving this solution in the closed vessels overnight at 80 °C before drying down again.

Elemental separation

Lu-Hf extraction was achieved by two cation-exchange resin methods, based on Münker *et al*. (2001) and Sprung *et al*. (2010) with some modifications. In order to avoid matrix effects and the Lu tail in the Hf cut, the three-stage separation scheme after Sprung *et al*. (2010) was applied for most samples. This procedure is listed in Table 2. Most of the matrix elements including Light Rare Earth Elements (LREE) were eluted sequentially with 2–3 M and 3M HCl. The solution was collected in 50 mL Teflon® PFA beakers and used for further element separation for other isotope systems like Sm-Nd or Rb-Sr. The HREE fraction was then eluted with 6 M HCl and evaporated to dryness. After HREE elution, the column was rinsed with 6M HCl. Subsequently, Ti

Table 1. Descriptions of selected analyzed samples.

Sample ID	Rock/Min type	Location	Age (~)Ma	Description	Reference values			
					Lu (ppm)¥	Hf (ppm)¥	$^{176}Lu/^{177}Hf$	$^{176}Hf/^{177}Hf$ ±2 S.D
USGS Reference rocks								
AGV-1	Andesite	Guano Valley, USA	16	Aphanitic, finely porphyritic, with a trachytic texture. Phenocrysts of Ol, Pl and Cpx.[1]	Range=0.24-0.25[12,13] Mean=0.25 (n=6)	Range=4.96-5.17[5,13] Mean=5.09 (n=4)	Range=0.00690-0.00696[13] Mean=0.00692 (n=3)	Range=0.282669-0.283000[4,6,7,13,19] Mean=0.282981±18 (n=13)
BCR-1	Basalt	Portland, USA	16	Aphanitic and hypocrystalline basalt with an interstitial texture of Pl laths, interstitial Px + Fe-oxides.[1]	Mean=0.51[12,13] (n=6)	Range=4.95-4.99[12-14] Mean=4.97 (n=7)	Range=0.01461-0.01469[12,13] Mean=0.01465 (n=6)	Range=0.282833-0.282896[6,8-16,24-27] Mean=0.282868±27 (n=35)
BHVO-1	Basalt	Kilauea, USA	<0.1	From the surface layer of the pahoehoe lava of Kilauea Crater.[1]	Range=0.24-0.28[7,12,13,1718] Mean=0.27 (n=16)	Range=3.93-4.68[5,7,12,13,17,18] Mean=4.41 (n=21)	Range=0.00878-0.00897[7,12,13,17,20] Mean=0.00884 (n=20)	Range=0.283076-0.283116[6-9,11-13,17-20,24,26,27] Mean=0.283102±18 (n=59)
BIR-1	Basalt	Reykjavi, Iceland	<0.1	Interglacial lava flows. The rock is a coarse-grained Ol tholeiite.[2]	Range=0.24-0.25[14,18,28] Mean=0.24 (n=11)	Range=0.56-0.69[14,18,28] Mean=0.59 (n=11)	Range=0.05184-0.06084[14,18,28] Mean=0.059106 (n=11)	Range=0.283239-0.283281[8,9,14,18,21,22,24,28] Mean=0.283271±37 (n=23)
G-2	Granite	Bradford, USA	520	Two mica granite, rich in Pl and Bt.[1]	Mean=0.10(n=12)[13,28]	Mean=8.04(n=12)[13,28]	Mean=0.00175(n=12)[13,28]	Range=0.282500-0.282532[6,13,28] Mean=0.282520±16 (n=21)
GSP-1	Granodio-rite	Silver Plume, USA	1,590	Medium grained hypidiomophic rock, consisting of Qtz + Pl + Bt + Ms + Kfs.[1]	Range=0.22-0.24[13] Mean=0.23 (n=2)	Range=16.05-16.47[13] Mean=16.26 (n=2)	Range=0.00195-0.00208[13] Mean=0.002017 (n=2)	Range=0.281910-0.281923[13] Mean=0.281917 (n=2)
GSJ Reference rocks								
JG-2	Granite	Gifu, Japan	100	Naegi granite (Biotite granite).[3]	—	—	Range=0.02872-0.03882[23] Mean=0.03344 (n=6)	Range=0.282546-0.282560[23] Mean=0.282554±12 (n=6)
JG-3	Granodio-rite	Simane, Japan	54	Mitoya granodiorite (Homblende - Biotite granodiorite).[3]	—	—	—	—
Chiapas Massif samples								
03-1b	Gneiss	Chiapas, Mex.	1,000	Boudins of felsic ortho-gneiss with granoblastic texture, consisting of Qtz + Pl + Bt + Kfs. [30]	—	—	—	—
03-2a	Gneiss	Chiapas, Mex.	1,000					
R0907	Schist	Chiapas, Mex.	450*	Pelitic schist highly deformed, dominated by Grt + Sil + Bt + Ms + Pl. Depleted in Zrn.[29]	—	—	—	—
03-2b	Metabasite	Chiapas, Mex.	450*	Metabasite with variable grade of migmatization,. It is composed of Pl + Hbl + Bt + Il + Qtz + Ap + Fe-oxides.[30]	—	—	—	—
03-2c	Metabasite	Chiapas, Mex.	450*					
05-1a	Metabasite	Chiapas, Mex.	450*					
Zrn-01	Zircon	Chiapas, Mex.	1,000	Grenvillian Zrn from 03-2a whole-rock sample.	—	—	—	—
Zrn-01	Zircon	Chiapas, Mex.	450*	Metamorphic Zrn from 03-2c whole-rock sample.	—	—	—	—
Zrn-02	Zircon	Chiapas, Mex.	1,000	Grenvillian xenocrystic Zrn from 03-2c whole-rock sample.	—	—	—	—
Zrn-03	Zircon	Chiapas, Mex.	1,000	Grenvillian xenocrystic Zrn from 03-2c whole-rock sample.	—	—	—	—
Zrn-04	Zircon	Chiapas, Mex.	1,000	Grenvillian xenocrystic Zrn from 03-2c whole-rock sample.	—	—	—	—
Anf-01	Amphibole	Chiapas, Mex.	—	Amp separated from sample 03-2c with an amperage between 0.2 and 0.4 at 15º in the Frantz table.	—	—	—	—
Anf-02	Amphibole	Chiapas, Mex.	—					
Anf-03	Amphibole	Chiapas, Mex.	—	Amp separated from sample 03-2c with an amperage between 1.0 and 2.0 at 5º in the Frantz table. Secondary grains.	—	—	—	—
Anf-04	Amphibole	Chiapas, Mex.	—					

Abbreviations: Amp, amphibole; Ap, apatite; Bt, biotite; Cpx, clinopiroxene; Grt, garnet; Hbl, hornblende; Il, ilmenite; Kfs, alkaline feldspar; Ms, muscovite; Ol, olivine; Pl, plagioclase; Px, pyroxene; Qtz, quartz; Sil, sillimanite; Zrn, zircon.¥ Reported from ID analyses. * Metamorphic age. References: [1]Flanagan (1967); [2]Flanagan (1984); [3]Ando and Shibata (1988); [4]Chauvel *et al.* (2010); [5]Lu *et al.* (2007); [6]Weis *et al*. (2007) ; [7]Pourmand and Dauphas (2010); [8]Bizarro *et al.* (2003); [9]Blichert-Toft (2001); [10]Chu *et al.* (2002); [11]Jochum *et al.* (2006); [12]Lapen *et al*. (2004); [13]Mahlen *et al.* (2008); [14]Münker *et al.* (2001); [15]Ulfbeck *et al*. (2003); [16]van de Flierdt *et al.* (2007); [17]Connelly *et al.* (2006); [18]Le Fèvre and Pin (2005); [19]Lu *et al.* (2007); [20]Vervoort *et al.* (2004); [21]Chu *et al*. (2011); [22]Hanyu *et al*. (2005); [23]Nebel *et al.* (2010); [24]Bizimis *et al*. (2005); [25]Ellam (2006); [26]Li *et al.* (2006);[27]Salters *et al.* (2011); [28]Bast *et al*. (2015); [29]Weber *et al*. (2008); [30]González-Guzmán *et al*. (2014).

Table 2. Three-stage HREE-Hf separation scheme based on Sprung *et al.* (2010) using ion-exchange chromatography of 1–1.2 mL of Eichrom Ln-Spec resin with 50–100 mesh; resin bed length: 3.8–4.0 cm.

Step	Volume (mL)	Reagent	Comment
Separation of Lu and Hf from matrix			
Clean	1R	6M HCl, 2M HF	Add some H_2O between the change of acid
Equilibrate resin	2 × 5	2-3M HCl	Pre-conditioned
Load sample,collect matrix	20	2-3M HCl	Could be collected for Sm-Nd analysis
Collect matrix	10	3M HCl	
Collect HREEs	12	6M HCl	Mainly Yb+Lu
Rinse HREEs off column	2 × 10	6M HCl	Remaining Lu
Rinse column	2 × 2	H_2O	Washout of resin
Rinse Ti+Nb off column	2-10 R	0.45M HNO3 +0.09M Hcit +1 vol %H2O2	Eluted with an orange to orange-red colour in column
Rinse column	2 × 2	H_2O	Washout of resin
Rinse Zr off column	3 × 10	6M HCl+0.06M HF	It can be cut or complete in Hf clean-up stage
Collect Hf	12	2M HF	
Clean	1R	6M HCl, 2M HF	Add some H_2O between Change of acid
Hf clean up			
Equilibrate resin	2 × 5	3M HCl	Pre-conditioned
Load sample	10	3M HCl+0.1M H_{asc}	H_{asc}reduces $Fe^{3+}$to Fe^{+2}
Rinse Fe off column	10	3M HCl	
Rinse HREEs off column	1-2 × 10	6M HCl	Remaining Lu
Rinse Zr off column	2 × 10	6M HCl+0.06M HF	Volume depending on the first 'Zr off' step
Collect Hf	12	2M HF	
Clean	1R	6M HCl	
Lu clean up			
Equilibrate resin	2 × 5	1M HCl	Pre-conditioned
Load sample	8	1M HCl+0.1M H_{asc}	Volume depending on resin mesh (5-10 mL)
Rinse Fe off column	10	1M HCl	H_{asc}reduces $Fe^{3+}$to Fe^{+2}
Collect Lu	12	6M HCl	
Clean	1R	6M HCl, 2M HF	Add some H_2O between the change of acid

R= Reservoir; here refers to column volume. The organic acid and H_2O_2reagent should be used fresh. The Ti+Nb separation step uses the acid volume necessary to achieve a colourless eluate and then another 5–10 additional mL.

was eluted using a mixture of 0.45 M HNO_3, 0.09 M citric acid (H_{Cit}), and 1 vol % of H_2O_2. Prior to Hf collection, Zr was extracted from the column with a mixture of 6 M HCl and 0.06 M HF. Finally, Hf was collected with 12 mL of 2 M HF in 30 mL Teflon® PFA beakers and gently evaporated to dryness.

Since Fe^{3+} was eluted together with Hf^{4+} in the first separation step, the Hf cut was loaded again to the previously cleaned column in a mixture of HCl and 0.1M ascorbic acid. Ascorbic acid reduces Fe^{3+} to Fe^{2+}, which was then rapidly eluted in the subsequent step. (To avoid the ascorbic acid in the LREE cut for further Sm-Nd or Rb-Sr separation, the sample was not loaded with ascorbic acid in the first separation step). The Hf clean-up was completed essentially in the same way as the first separation procedure except for the Ti elution that was omitted. This procedure reduced significantly Lu+Yb interferences on the ^{176}Hf signal. Finally the Lu cut was loaded with ascorbic acid to the precleaned columns to further reduce the Yb/Lu. It is important to note that this chemical separation method is time-consuming and the oxidation procedure (Ti elution step) can result in strong reactions that may lead to loss or cross-contamination of samples by ejecting material.

Mass spectrometry

The determination of Lu and Hf isotope ratios was carried out on a Thermo Neptune Plus® MC-ICP-MS installed at the Centro de Geociencias, Universidad Nacional Autonóma de México, in Juriquilla, Querétaro. All masses were measured on Faraday cups in static mode. The cup configuration is summarized in Table 3 and the typical signals are depicted in Figure 1. The sample solutions were introduced to the plasma via an Aridus® desolvating sample introduction system using an Ar carrier gas and a blended Ar + N_2 sweep gas. The beam intensities were then optimized by adjusting the torch position, gas flows, ion focusing, and magnet field settings. The Hf fraction was taken up with 1 mL of 0.56 M HNO_3–0.24 M HF solution and the Lu fraction from 0.6 mL of 0.1 M HNO_3 solution.

The isotope concentrations of Hf and Lu in the sample solutions were estimated by measuring peak sizes of diluted sample fractions prior to isotope data acquisition to make sure that signals are not too high to saturate the Faraday cups. Samples were then adjusted to ~50 ppb for Hf and ~10 ppb for Lu isotope analyses. Washouts were performed with MQ Water and 0.45 M HNO_3-HF trace for 120–240 seconds or until all signal intensities were below 5×10^{-4} V. Baselines

Table 3. Faraday cup configurations for Lu and Hf isotope analysis using Neptune® MC-ICP-MS.

Faraday Cup	L4	L3	L2	L1	Center	H1	H2	H3	H4
Lu configuration									
Mass	170	172	173	174	175	176	177	185	187
Isotopes	^{170}Yb	^{172}Yb	^{173}Yb	^{174}Yb ^{174}Hf	^{175}Lu	^{176}Yb ^{176}Lu ^{176}Hf	^{177}Hf	^{185}Re	^{187}Re
Hf configuration									
Mass	172	174	175	176	177	179	180	181	182
Isotopes	^{172}Yb	^{174}Yb ^{174}Hf	^{175}Yb	^{176}Yb ^{176}Lu ^{176}Hf	^{177}Hf	^{179}Hf	^{180}Hf ^{180}Ta ^{180}W	^{181}Ta	^{182}W

were acquired measuring backgrounds at peak positions (on-peak-zeroes, OPZ) at least twice during each analytical session, using the same acid solution used for the washouts. The OPZ intensities were subtracted from the corresponding peaks when the baseline intensities were higher than 5×10^{-4} V.

Lu isotope analysis

For Lu isotope data acquisition one block of 40 cycles with 4 seconds integration time each was performed. The ^{177}Hf intensity was measured to monitor for isobaric interference of ^{176}Hf on the ^{176}Lu signal. For the mass bias correction, each sample was doped with ~10 ppb of Re and the masses 185 and 187 were measured simultaneously on cups H3 and H4 (Table 3). Lu-Re (10 ppb Lu + 15 ppb Re) and/or Yb-Lu-Re (10 ppb Yb + 10 ppb Lu +15 ppb Re) standard solutions were measured after every 3–5 unknowns to account for differences in instrumental mass bias between the elements.

Hf isotope analysis

For Hf isotope data acquisition 8 blocks with 10 cycles per block and an integration time of 4 seconds per cycle were measured. Isobaric interferences of ^{176}Yb and ^{176}Lu on the ^{176}Hf signal were monitored by measuring ^{172}Yb and ^{175}Lu. Moreover, ^{181}Ta and ^{182}W were measured to monitor for isobaric interferences of ^{180}Ta and ^{180}W on the spiked isotope ^{180}Hf (Table 3). The interference correction was calculated from the known natural ratio of the isotopes from the interfering element.

To examine the accuracy of Hf isotope measurement, a 50 ppb JMC 475 Hf standard solution was measured after every 4-5 unknowns. The average ^{176}Hf/^{177}Hf ratio of JMC 475 measured over the last three years during a total of six analytical sessions is 0.282149 ± 0.000025 (n = 41), which is slightly below but within errors of cited values (*e.g.*, Blichert-Toft *et al.*, 1997: 0.282163 ± 0.000009; Münker *et al.*, 2001: 0.282151 ± 0.000013; Lapen *et al.*, 2004: 0.282165 ± 0.000013; Vervoort *et al.*, 2004: 0.282144 ± 0.000014, all errors are 2S.D). Therefore, all measured ^{176}Hf/^{177}Hf ratios were normalized to the well-accepted JMC 475 value of 0.282160. The results of the JMC 475 standard measurements are shown in Figure 2.

DATA REDUCTION

For offline reduction of the raw data extracted from the mass spectrometer, an R-based software package (CRAN) was written. The Hf isotope data reduction Toolkit for R (in short: IsotopeHf®) can be requested from the corresponding author. This contribution aims to introduce this package, with integrated functions for data corrections, calculation, and graphical output, focused on determining elemental concentrations and isotopic ratios for Lu and Hf, as well as the corresponding uncertainties. It is important to note that IsotopeHf® is a cross-platform program that can be run on any operating system with R environment installed (version 3.1.1 or later). For a proper functionality of IsotopeHf® other packages (CRANs) must be installed; namely "ggplot2", "plyr", and "dplyr" (Wickham, 2009; Wickham, 2011; Wickham and Francois, 2015). IsotopeHf® runs via the command-line interface. The user's guide is included in the Appendix of this paper (Electronic Supplementary File) and it can be displayed within the program. Advantages, disadvantages and known bugs of IsotopeHf® are listed in Table 4. In the following sections, the main equations used in IsotopeHf® to correct the raw data from the Lu and Hf data acquisition by MC-ICP-MS are explained.

Lu isobaric interference correction (and Yb mass bias correction)

Isobaric interferences for ^{176}Lu occur with ^{176}Yb and ^{176}Hf. After the three-stage elemental separation procedure employed in this study that includes a Lu clean-up procedure, the ^{176}Hf interference is insignificant. However, Yb and Lu show similar adsorption behavior on Ln-Spec® resin and are difficult to separate from each other. Therefore, the contribution of ^{176}Yb on the 176 mass peak has to be corrected, considering also the mass bias for Yb isotope ratios. In a first step for isobaric interference correction on ^{176}Lu, the Yb mass bias factor β_{Yb} is calculated applying the exponential law (Russell *et al.*, 1978) as follows:

$$\beta_{Yb} = \ln\left[\frac{\left(\frac{^{172}Yb}{^{173}Yb}\right)_{Mea}}{\left(\frac{^{172}Yb}{^{173}Yb}\right)_{Nat}}\right] \div \ln\left[\frac{Mass(^{172}Yb)}{Mass(^{173}Yb)}\right] \quad (1)$$

Then, the interference corrected $^{176}Lu_{IC}$ signal is calculated by subtracting the mass bias corrected ^{176}Yb fraction from the measured 176 mass signal using the equation (Vervoort *et al.*, 2004):

$$^{176}Lu_{IC} = {}^{176}(Lu+Yb)_{Mea} - \left[{}^{173}(Yb)_{Mea} \times \left(\frac{^{176}Yb}{^{173}Yb}\right)_{Nat} \times \left[\frac{Mass(^{173}Yb)}{Mass(^{176}Yb)}\right]^{\beta_{Yb}}\right] \quad (2)$$

where the subscripts IC, Mea, and Nat are interference corrected, measured, and natural, respectively. To correct for mass bias of Yb and to calculate its isobaric contribution on ^{176}Lu, natural Yb isotope compositions reported by Segal *et al.* (2003) were used (^{172}Yb/^{173}Yb = 1.35428 and ^{176}Yb/^{173}Yb = 0.79381). It is noteworthy that Vervoort *et al.* (2004) noted an over-correction of the ^{176}Lu/^{175}Lu values by subtracting the ^{176}Yb interference from ^{176}Lu using this protocol. To solve this, an empirical correction factor (typically 0.9996, Vervoort *et al.,*

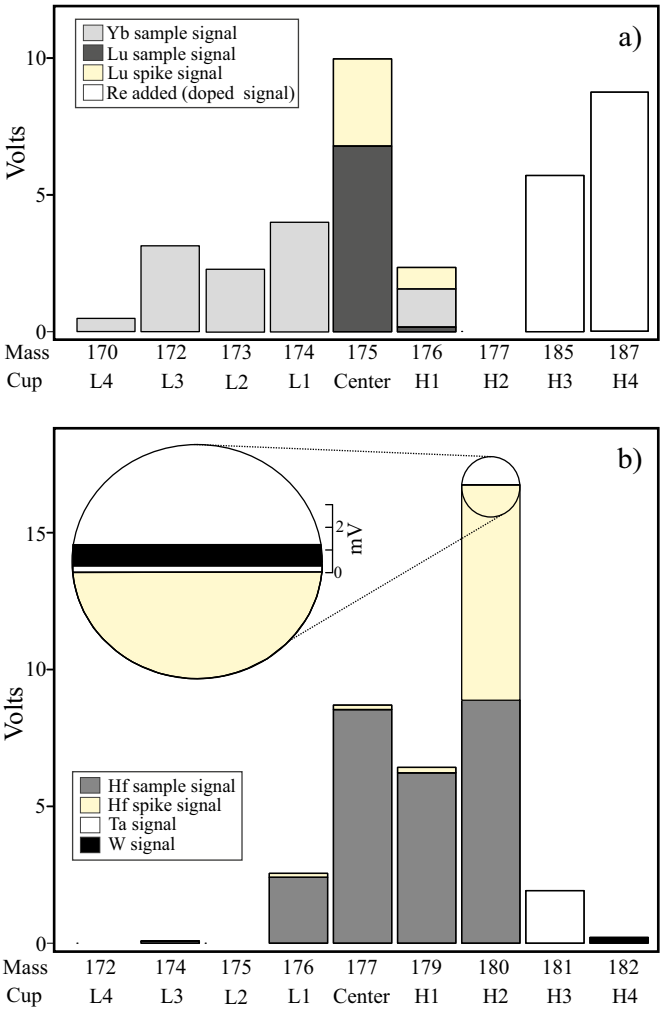

Figure 1. Bar chart illustrating the relative contributions of spike and sample components for typical MC-ICP-MS Lu-Hf analyses. (a) Typical signals for the Lu analysis and (b) typical signals for the Hf analysis. Notice the minimal ^{180}Ta and ^{180}W contribution on ^{180}Hf.

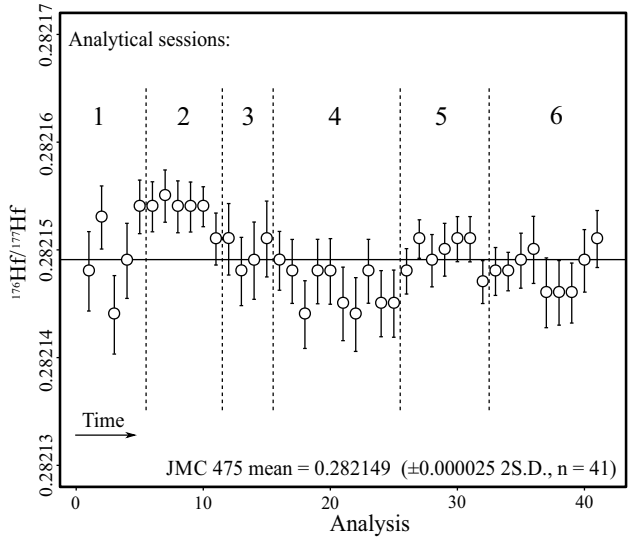

Figure 2. Measured ^{176}Hf/^{177}Hf ratios of 50 ppb Hf standard solution JMC 475. Horizontal line shows the mean and vertical dashed lines separate analytical sessions. Error bars are 2S.E. on measurement.

2004) can be used to adjust $(^{173}Yb/^{176}Yb)_{Nat}$ in Equation 2. Our mixed Lu-Yb-Re standard solution (with Yb/Lu = 1) yielded ^{176}Lu/^{175}Lu ranging from 0.02651 to 0.02655 (mean = 0.02653 ± 0.00002 2S.D., n=14). These values correspond within analytical uncertainties to the natural isotopic composition of Lu reported by several authors (Blichert-Toft *et al.*, 1997; Chu *et al.*, 2002; Kleinhanns *et al.*, 2002; Vervoort *et al.*, 2004, Figure 3a). Considering that the chemical separation method after Sprung *et al.* (2010) decreases the Yb/Lu value to about 1 in the Lu cut and that ^{176}Lu/^{175}Lu remained constant on the Neptune® MC-ICP-MS over the whole period of analysis (three years), an additional correction factor as proposed by Vervoort *et al.* (2004) was not necessary, at least in this study.

Lu mass bias correction

Instrumental mass bias behavior of Lu cannot be determined by using the natural constant isotope ratio, because Lu has only two naturally occurring isotopes (^{175}Lu and ^{176}Lu), of which the ^{176}Lu signal is altered by the spike isotope. The mass bias can be corrected by normalizing to an external standard of known isotopic composition that is simultaneously measured with the multi-collector system. For this purpose the samples were doped with admixed Re (see Figure 1a). The doping method has been successfully employed for mass-bias correction in many isotope systems, such as Cu isotopes with admixed Zn (Maréchal *et al.*, 1999), Rb isotopes with admixed Zr (Nebel *et al.*, 2005), and Lu isotopes with admixed W (Wimpenny *et al.*, 2013).

Rhenium is ideal as doping agent for Lu measurements, since its isotope mass range is close to that of Lu and it contains no isobaric interferences. Rhenium doping was first introduced by Scherer *et al.* (1999) and applied in several Lu-Hf studies (*e.g.*, Münker *et al.*, 2001; Scherer *et al.*, 2001; Kleinhanns *et al.*, 2002; Weber *et al.*, 2010; Wimpenny *et al.*, 2013). The method is based on the assumption that instrumental mass bias of Re and Lu in MC-ICP-MS does not vary independently in the same solution at the same time. Hence, this behavior can be used to cross-calibrate the mass bias factors (β). The relation between mass bias factors obtained with the exponential law can be calculated from the slope (m) of the linear array plotted in $\ln(^{187}Re/^{185}Re)$ *vs.* $\ln(^{176}Lu/^{175}Lu)$ (Figure 4):

$$m = \frac{\beta_{Lu}}{\beta_{Re}} \times \left[\frac{\ln\left[\frac{Mass(^{176}Lu)}{Mass(^{175}Lu)}\right]}{\ln\left[\frac{Mass(^{187}Re)}{Mass(^{185}Re)}\right]} \right] \quad (3)$$

The regression line with the slope (m) is calculated from standard solutions containing both Re and natural Lu, which were measured during a working session after every 3–5 unknowns. The property of the linear array still holds in the unknown sample solutions, inasmuch as their two mass bias factors (β_{Re} and β_{Lu}) are proportional throughout the working session. We first calculated β_{Re} in the sample:

$$\beta_{Re} = \ln\left[\frac{\left(\frac{^{187}Re}{^{185}Re}\right)_{Nat}}{\left(\frac{^{187}Re}{^{185}Re}\right)_{Mea}} \right] \div \ln\left[\frac{Mass(^{187}Re)}{Mass(^{185}Re)}\right] \quad (4)$$

Then, β_{Lu} is calculated from the β_{Re} [Equation 4, $(^{187}Re/^{185}Re)_{Nat}$ = 1.67398 after Gramlich *et al.*, 1973] and from the slope (m) of the linear array of the log-log plot.

Table 4. Avantages, disadvantages and known bugs of IsotopeHf®.

Advantages	Disadvantages and known bugs
Runs in any operating system with R environment installed (version >=3.1.1).	No own graphical user interface (GUI).
Reads *.FIN2 and csv files.	Basic knowledge is needed on R language.
Detects and shows outlier values.	The package was develop to a specific MC-ICP-MS program and cup configuration (see Figure 1).
The data reduction functions display a graphic output.	To change some default values (*e.g.*, spike, masses, CHUR), it is necessary to know the source code.
Users are free to study, change and improve the source code for your own requirements.	There are some conflicts between "plyr" (Wickham, 2011) and "dplyr" (Wickham and Francois, 2015) as dependent packages.
An extensive documentation is included in the package.	

*output file from Thermo Neptune® MC-ICP-MS.

$$\beta_{Lu} = m \times \left[\frac{\ln\left[\frac{\text{Mass}(^{187}\text{Re})}{\text{Mass}(^{185}\text{Re})}\right]}{\ln\left[\frac{\text{Mass}(^{176}\text{Lu})}{\text{Mass}(^{175}\text{Lu})}\right]} \right] \times \beta_{Re} \quad (5)$$

Finally, the mass bias corrected $^{176}Lu/^{175}Lu$ is calculated by using the interference corrected ^{176}Lu and β_{Lu}.

$$\left(\frac{^{176}\text{Lu}}{^{175}\text{Lu}}\right)_{IC+MB} = \frac{^{176}\text{Lu}_{IC}}{^{175}\text{Lu}} \times \left[\frac{\text{Mass}(^{176}\text{Lu})}{\text{Mass}(^{175}\text{Lu})}\right]^{\beta_{Lu}} \quad (6)$$

where the subscripts MB and IC are mass bias corrected and interference corrected, respectively.

The Re doping method is an approach that deals with the problem that Lu and Yb do not fractionate equally. Besides that the differences between the mass bias factors may vary from one instrument to another, from one analytical session to another, and also during a long analytical session (>16 h). Variations in the Yb and Lu mass bias factors (β) during two different analytical sessions are depicted in Figure 3b.

Hf mass bias correction and correction for spike

Correction of $^{176}Hf/^{177}Hf$ for mass bias in unspiked samples is usually achieved by normalizing to the accepted natural $^{179}Hf/^{177}Hf$ of 0.7325. Due to alteration of the natural isotope ratios by the admixed isotope tracer that is never 100% pure spike isotope, correction with natural $^{179}Hf/^{177}Hf$ is inaccurate. Thus the "True" $^{179}Hf/^{177}Hf$ for the mixed solution needs to be calculated. Besides that, for the interference correction of ^{176}Lu on ^{176}Hf by using the ^{175}Lu monitor, the measured and corrected $^{175}Lu/^{176}Lu$ has to be used, since this isotope ratio is also altered by the spike. This can introduce an additional systematic error on the resulting $^{176}Hf/^{177}Hf$ if a significant Lu-tail is present in the Hf cut.

Several approaches have been suggested to correct the $^{176}Hf/^{177}Hf$ in spiked samples. Lapen *et al.* (2004) used closed-form equations, modified from the double-spike approach that simultaneously provides a solution for the spike and mass-bias corrections on $^{176}Hf/^{177}Hf$. However, Lapen *et al.* (2004) used a spike enriched in ^{178}Hf, and they used the $^{180}Hf/^{177}Hf$ to test the reliability of the correction method. Such an approach will need long-term comparison to external reproducibility of both unspiked and spiked samples. On the other hand, Lu *et al.* (2007) reported an iterative solution for a simultaneous determination of the Hf concentration and $^{176}Hf/^{177}Hf$ ratio using a spike enriched in ^{179}Hf, yielding identical analytical results in both spiked and unspiked samples of geochemical reference standards. The Hf concentration is derived from the spike-to-sample molar ratio. Sprung *et al.* (2010) preferred a $^{179}Hf/^{177}Hf$-normalized procedure derived from considerations of Maréchal *et al.* (1999), by using the linear trend of

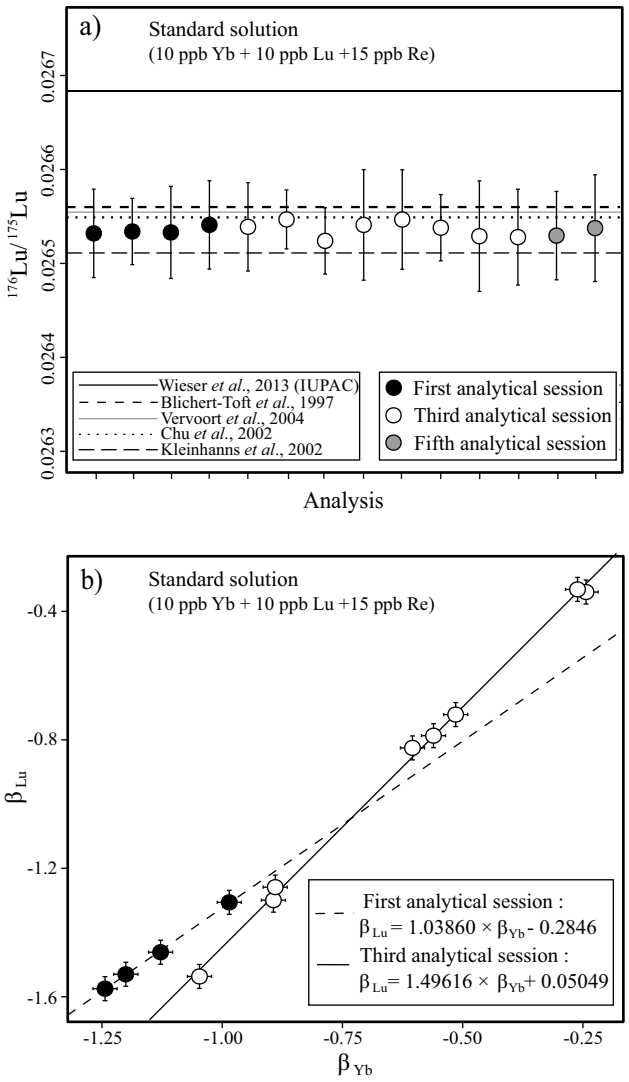

Figure 3. (a) Relationship between $^{176}Lu/^{175}Lu$ corrected for mass bias + Yb interference on mixed Yb+Lu+Re solution in some analytical sessions and true $^{176}Lu/^{175}Lu$ reported by Blichert-Toft *et al.* (1997); Chu *et al.* (2002); Kleinhanns *et al.* (2002); Vervoort *et al.* (2004) and Wieser *et al.* (2013). (b) Variations of mass bias between Yb and Lu during two analytical sessions. The mass-bias factors were characterized using Yb + Lu + Re solution. β_{Yb} was calculated by Equation 1. β_{Lu} was calculated by Re-Lu doping method.

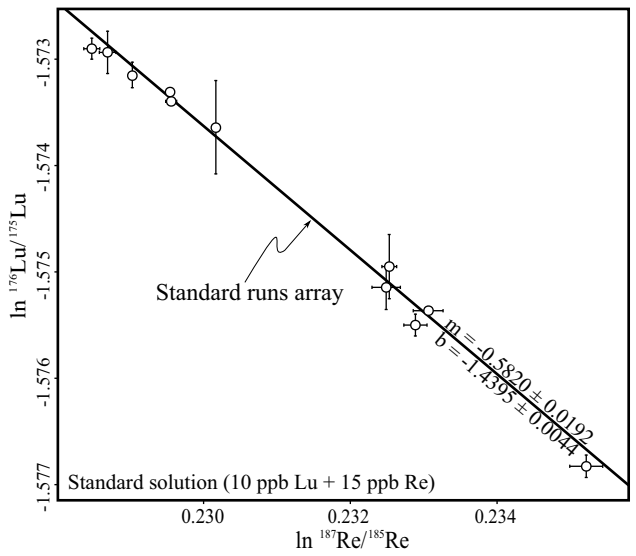

Figure 4. Re *vs.* Lu log-log plot showing the slope (m) obtained from the external isotopic standard (Lu + Re solution) during a typical Lu working session. This slope is used to correct for Lu sample + Re standard mixtures. The two mass bias factors (β_{Re} and β_{Lu}) are proportional throughout the working session. The errors bars represent 2S.D.

the measured Hf standard solutions to cross-calibrate the mass bias factors (β) of the samples.

For the IsotopeHf® software an empirical method based on the equations of Boelrijk (1968), Qiao (1988), and Gopalan (2002), and developed by Chu *et al.* (2011) was applied, first obtaining the spike contribution on $^{179}Hf/^{177}Hf$, then using the spike-corrected $^{179}Hf/^{177}Hf$ to calculate the mass bias factor (β_{Hf}), and finally correcting the effects of both spike and mass bias on the $^{176}Hf/^{177}Hf$.

In a first step, the interference corrections of ^{180}Ta and ^{180}W on the ^{180}Hf signal (close-up in Figure 1b) are calculated:

$$^{180}Hf_{IC} = {}^{180}(Hf + Ta + W)_{Mea} - \left(\left[\left(\frac{^{180}Ta}{^{181}Ta}\right)_{Nat} \times (^{181}Ta)_{Mea}\right] + \left[\left(\frac{^{180}W}{^{182}W}\right)_{Nat} \times (^{182}W)_{Mea}\right]\right) \quad (7)$$

Since the mass bias cannot be corrected without considering the spike, the contribution of the spike in the sample ($D = {}^{177}N_{Sp}/{}^{177}N_{Nat}$) is calculated:

$$D = \frac{^{177}N_{Sp}}{^{177}N_{Nat}} = \frac{\left(\frac{^{180}Hf}{^{177}Hf}\right)_{Nat} - \left(\frac{^{180}Hf}{^{177}Hf}\right)_{IC+MB}}{\left(\frac{^{180}Hf}{^{177}Hf}\right)_{IC+MB} - \left(\frac{^{180}Hf}{^{177}Hf}\right)_{Sp}} \approx \frac{\left(\frac{^{180}Hf}{^{177}Hf}\right)_{Nat} - \left(\frac{^{180}Hf}{^{177}Hf}\right)_{IC}}{\left(\frac{^{180}Hf}{^{177}Hf}\right)_{IC} - \left(\frac{^{180}Hf}{^{177}Hf}\right)_{Sp}} \quad (8)$$

where ^{177}N is the number of moles of ^{177}Hf, and the subscripts Nat, Sp, IC, and MB are for natural, spike, interference corrected, and mass bias corrected, respectively. Although the spike used in this study is artificially enriched in the ^{180}Hf isotope to more than 98%, the spike contribution on the $^{179}Hf/^{177}Hf$ and $^{176}Hf/^{177}Hf$ is significant and needs to be corrected using the following equations:

$$\left(\frac{^{179}Hf}{^{177}Hf}\right)_{SC} = \left(\frac{^{179}Hf}{^{177}Hf}\right)_{Mea} + \left[\left(\frac{^{179}Hf}{^{177}Hf}\right)_{Mea} - \left(\frac{^{179}Hf}{^{177}Hf}\right)_{Sp}\right] \times D \quad (9)$$

$$\left(\frac{^{176}Hf}{^{177}Hf}\right)_{SC} = \left(\frac{^{176}Hf}{^{177}Hf}\right)_{Mea} + \left[\left(\frac{^{176}Hf}{^{177}Hf}\right)_{Mea} - \left(\frac{^{176}Hf}{^{177}Hf}\right)_{Sp}\right] \times D \quad (10)$$

where the subscripts SC and Mea are spike corrected and measured, respectively. Herewith, the mass bias factor (β_{Hf}) is obtained from the $^{179}Hf/^{177}Hf$ without the contribution of the spike after

$$\beta_{Hf} = \ln\left[\frac{\left(\frac{^{179}Hf}{^{177}Hf}\right)_{SC}}{\left(\frac{^{179}Hf}{^{177}Hf}\right)_{Nat}}\right] \div \ln\left[\frac{Mass(^{179}Hf)}{Mass(^{177}Hf)}\right] \quad (11)$$

to finally correct the $^{176}Hf/^{177}Hf$ and $^{180}Hf/^{177}Hf$ for mass bias.

$$\left(\frac{^{176}Hf}{^{177}Hf}\right)_{SC+MB} = \left(\frac{^{176}Hf}{^{177}Hf}\right)_{SC} \times \left[\frac{Mass(^{177}Hf)}{Mass(^{176}Hf)}\right]^{\beta_{Hf}} \quad (12)$$

$$\left(\frac{^{180}Hf}{^{177}Hf}\right)_{IC+MB} = \left(\frac{^{180}Hf}{^{177}Hf}\right)_{IC} \times \left[\frac{Mass(^{177}Hf)}{Mass(^{180}Hf)}\right]^{\beta_{Hf}} \quad (13)$$

A test for the correct spike subtraction is obtained by comparing the mass bias and spike corrected $^{179}Hf/^{177}Hf$ relative to the accepted natural value (0.7325).

$$\left(\frac{^{179}Hf}{^{177}Hf}\right)_{Nat} = \left(\frac{^{179}Hf}{^{177}Hf}\right)_{SC+MB} = \left(\frac{^{179}Hf}{^{177}Hf}\right)_{SC} \times \left[\frac{Mass(^{177}Hf)}{Mass(^{179}Hf)}\right]^{\beta_{Hf}} \quad (14)$$

RESULTS AND DISCUSSION

The corrected Lu-Hf isotope ratios and elemental compositions for international reference rock standards, unknown whole-rock, and mineral samples are listed in Table 5. Deviations of the obtained data from the recommended values for reference standard (from Table 1) as well as differences between the Parr® and the DAS® digestion methods and replicate analyses for both reference standard and unknown rock samples are listed.

The precision of the analytical procedure and reduction algorithms used by IsotopeHf® for mafic rocks (n=5, unknowns and standards), is illustrated in Figure 5 comparing the results from duplicate analysis using DAS® pressure digestion system. The duplicates show good agreement, yielding correlation coefficients (R^2) of 0.9970 for $^{176}Hf/^{177}Hf$ (Figure 5a) and 0.9992 for Lu/Hf, respectively (Figure 5b).

Validation of the separation technique

The quality of Hf separation from Yb and Lu is indicated by $^{172}Yb/^{176}\Sigma$ and $^{175}Lu/^{176}\Sigma$ values below 0.0001 (Bast *et al.*, 2015), which was the case for all whole-rock samples separated with the three-stage separation scheme that included an additional Hf clean-up (after Sprung *et al.*, 2010, Figure 6). Samples separated with the single column procedure (Münker *et al.*, 2001) occasionally show significant Yb and Lu-tails in the Hf cuts ($^{172}Yb/^{176}\Sigma$ up to 0.0118 and $^{175}Lu/^{176}\Sigma$ up to 0.0113, Figure 6). The necessary correction for ^{176}Lu increases significantly the error on $^{176}Hf/^{177}Hf$, especially because the measured $^{175}Lu/^{176}Lu$ for spiked Lu and its corresponding error has to be consid-

Table 5. Lu-Hf isotope and concentration data of analyzed samples. Comparisons between replicate analysis and between this study and reference values

Sample ID	Methods[¥]	$^{176}Hf/^{177}Hf$ (±1S.D.)£	εHf (±2S.E.)[Π]	Lu (ppm)	Hf (ppm)	$^{176}Lu/^{177}Hf$[§]	Monitor in Hf aliquot			Δ from duplicate analysis				Δ from reference values (average)			
							n^{n}	$^{172}Yb/^{176}\Sigma^{*}$	$^{175}Lu/^{176}\Sigma^{*}$	%Δ Lu	%Δ Hf	%Δ $^{176}Lu/^{177}Hf$	Δ εHf	%Δ Lu	%Δ Hf	%Δ $^{176}Lu/^{177}Hf$	Δ εHf
Reference rocks																	
AGV-1(v1)	1,a	0.282968 (12)	6.43 (0.10)	0.24	5.18	0.00666	78	0.00058	0.00023	4.0	0.8	3.6	0.47	-4.0	1.8	-3.8	-0.50
AGV-1(v2)	1,b	0.282980 (9)	6.90 (0.07)	0.25	5.14	0.00691	78	0.00005	0.00006	51.0				0.0	1.0	-0.1	-0.03
BCR-1	1,a	0.282865 (13)	2.83 (0.10)	0.51	4.95	0.01463	79	0.00149	0.00076	—	—	—	—	0.0	-0.4	-0.1	-0.11
BHVO-1(v1)	1,a	0.283103 (14)	11.25 (0.11)	0.28	4.49	0.00889	77	0.00086	0.00079	3.7	1.4	2.3	0.21	3.7	1.8	0.6	0.04
BHVO-1(v2)	1,b	0.283109 (13)	11.46 (0.10)	0.27	4.43	0.00869	78	0.00004	0.00004					0.0	0.5	-1.7	0.25
BIR-1	1,a	0.283271 (22)	17.19 (0.18)	0.28	0.59	0.06659	77	0.00067	0.00039	—	—	—	—	16.6	0.0	12.7	0.27
G-2(v1)	2,b	0.282508 (13)	-9.80 (0.10)	0.10	8.25	0.00180	77	0.00003	0.00005	0.0	1.9	2.3	0.22	0.0	1.8	4.0	0.53
G-2(v2)	1,a	0.282514 (13)	-9.58 (0.10)	0.10	8.10	0.00176	78	0.00032	0.00036					0.0	0.0	1.0	0.31
GSP-1(v1)	2,b	0.281901 (19)	-31.26 (0.15)	0.24	15.40	0.00219	78	0.00002	0.00003	20.0	2.6	13.5	0.57	4.3	-5.3	8.4	-0.57
GSP-1(v2)	1,b	0.281917 (18)	-30.69 (0.15)	0.20	15.01	0.00193	78	0.00001	0.00001					-13.0	-7.7	-4.5	0.00
JG-2(v1)	2,b	0.282536 (13)	-8.81 (0.10)	1.28	4.72	0.03854	79	0.00002	0.00003	7.6	4.4	2.8	0.29	—	—	15.3	-0.64
JG-2(v2)	1,b	0.282544 (13)	-8.52 (0.10)	1.19	4.52	0.03748	78	0.00002	0.00002					—	—	12.1	-0.35
JG-3(v1)	2,b	0.282840 (18)	1.94 (0.15)	0.64	4.94	0.01846	77	0.00003	0.00004	16.4	6.9	8.1	0.22	—	—	—	—
JG-3(v2)	1,b	0.282846 (13)	2.16 (0.10)	0.55	4.62	0.01707	77	0.00001	0.00002					—	—	—	—
Unknown whole-rock samples																	
03-1b(v1)	2,b	0.282261 (12)	-18.53 (0.10)	0.62	25.64	0.00345	78	0.00002	0.00002	19.2	46.3	19.0	0.11	—	—	—	—
03-1b(v2)	1,b	0.282264 (13)	-18.42 (0.10)	0.52	17.53	0.00426	78	0.00007	0.00006					—	—	—	—
03-2a(v1)	2,b	0.282254 (9)	-18.78 (0.07)	0.59	28.72	0.00291	78	0.00002	0.00004	11.3	94.2	43.3	0.25	—	—	—	—
03-2a(v2)	1,a	0.282261 (18)	-18.53 (0.14)	0.53	14.79	0.00513	79	0.00082	0.00038					—	—	—	—
R0907(v1)	2,b	0.282560 (13)	-7.96 (0.10)	0.93	6.99	0.01891	79	0.00620	0.00257	8.6	4.3	4.4	0.04	—	—	—	—
R0907(v2)	1,a	0.282561 (18)	-7.92 (0.15)	1.01	7.29	0.01974	77	0.00012	0.00009					—	—	—	—
03-2b (v1)	1,a	0.282894 (12)	3.85 (0.10)	0.33	1.93	0.02413	77	0.00024	0.00020	3.1	1.6	2.0	0.11	—	—	—	—
03-2b (v2)	1,b	0.282897 (19)	3.96 (0.15)	0.32	1.90	0.02366	78	0.00006	0.00005					—	—	—	—
03-2c (v1)	1,a	0.282909 (18)	4.38 (0.14)	0.31	1.83	0.02429	79	0.00037	0.00036	0.0	0.0	1.0	0.17	—	—	—	—
03-2c (v2)	1,b	0.282904 (18)	4.21 (0.14)	0.31	1.83	0.02454	78	0.00005	0.00004					—	—	—	—
05-1a (v1)	1,a	0.282889 (13)	3.68 (0.10)	0.54	3.35	0.02291	78	0.00013	0.00015	0.0	0.0	0.4	0.07	—	—	—	—
05-1a (v2)	1,b	0.282891 (14)	3.75 (0.11)	0.54	3.35	0.02300	77	0.00002	0.00003					—	—	—	—
Mineral samples																	
03-2a(Zrn-01)	2,c	0.282180 (27)	-21.39 (0.21)	—	—	0.00063	77	0.00004	0.00005	—	—	—	—	—	—	—	—
03-2c(Zrn-01)	2,c	0.282708 (25)	-2.72 (0.19)	—	—	0.00037	78	0.00016	0.00016	—	—	—	—	—	—	—	—
03-2c(Zrn-02)	2,c	0.282213 (19)	-20.23 (0.14)	—	—	0.00069	76	0.00002	0.00006	—	—	—	—	—	—	—	—
03-2c(Zrn-03)	2,c	0.282250 (59)	-18.92 (0.46)	—	—	0.00108	78	0.00005	0.00004	—	—	—	—	—	—	—	—
03-2c(Zrn-04)	2,c	0.282204 (25)	-20.55 (0.21)	—	—	0.00028	76	0.00011	0.00007	—	—	—	—	—	—	—	—
03-2c(Anf-01)	1,b	0.282992 (9)	7.32 (0.07)	—	—	0.03324	78	0.00003	0.00003	—	—	—	—	—	—	—	—
03-2c(Anf-02)	1,b	0.282968 (26)	6.47 (0.21)	—	—	0.03017	79	0.00005	0.00004	—	—	—	—	—	—	—	—
03-2c(Anf-03)	1,b	0.282894 (16)	3.85 (0.13)	—	—	0.02008	77	0.00002	0.00004	—	—	—	—	—	—	—	—
03-2c(Anf-04)	1,b	0.282910 (13)	4.42 (0.11)	—	—	0.02070	77	0.00026	0.00013	—	—	—	—	—	—	—	—

[¥]Digestion method: 1=DAS[®] system, 2=Parr[®] bomb. Separation method: a = Münker *et al.* (2001), b = Sprung *et al.* (2010), c = Nebel-Jacobsen *et al.* (2005).
[£]Errors refer to the last digit(s) and are one standard deviations. [Π] Errors refer to the last digits and are 2S.E. = $2\sigma/\sqrt{n}$. [§]The $^{176}Lu/^{177}Hf$ errors are typically < 0.2% (2σ).
[n]Number of measured isotope ratios after outlier rejection. *Isotope ratios measured in Hf aliquot. $^{176}\Sigma = {}^{176}Yb + {}^{176}Lu + {}^{176}Hf$
The εHf values were calculated following CHUR $^{176}Hf/^{177}Hf$ value = 0.282785 (Bouvier *et al.*, 2008).

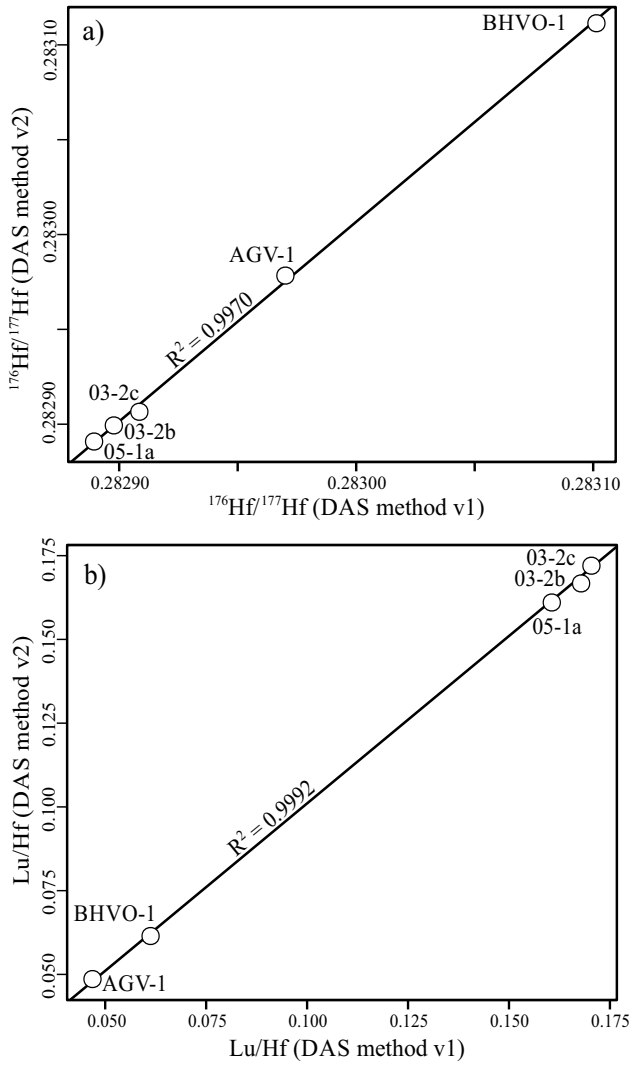

Figure 5. Comparison between results of (a) $^{176}Hf/^{177}Hf$ and (b) Lu/Hf on duplicate analyses of mafic rocks using DAS® system.

ered for the correction. However, after running data reduction with IsotopeHf® there is no significant difference on the resulting εHf values, neither for the reference standard with the highest $^{175}Lu/^{176}\Sigma$ of 0.00079 (BHVO-$1_{(v1)}$, ΔεHf = 0.04, Table 5), indicating that interference correction including the spike works properly with IsotopeHf®.

Accuracy and reproducibility of Hf-isotope ratios

The corrected $^{176}Hf/^{177}Hf$ values of international reference rock standards calculated with IsotopeHf® are accurate within analytical uncertainties with most published data (Figure 7). All standard basalts analyzed in this work (Figure 7a, 7b and 7d) yield $^{176}Hf/^{177}Hf$ values that deviate from the average reported values by less than 0.00001, corresponding to less that 0.3 εHf-units (BCR-1 = -0.11, BHVO-1 = from 0.04 to 0.25, BIR-1 = 0.27 εHf-units). One analysis of the standard andesite AGV-1 yielded a $^{176}Hf/^{177}Hf$ that is slightly lower (by -0.50 εHf-units) than the average but still within analytical errors of most reported values (Figure 7c).

Granitic reference rock standards are much more problematic, because $^{176}Hf/^{177}Hf$ values of the G-2, GSP-1, and JG-2 standards are poorly reported in literature and because the reported data are highly disperse (Mahlen *et al.*, 2008; Bast *et al.*, 2015, Figure 7e–7g). However, the corrected $^{176}Hf/^{177}Hf$ values of standard granitoids G-2, GSP-1, and JG-2 analyzed here do not differ from the reported values by more than 0.64 εHf-units. It is noteworthy that we report the first Lu-Hf isotope data for granodiorite standard JG-3.

The external reproducibility for $^{176}Hf/^{177}Hf$ of all analyzed samples ranges between 0.00 and 0.57 εHf-units but only two out of twelve duplicate analyses differ by more than 0.3 εHf-units: (1) Granodiorite standard GSP-1 (Δ = -0.57 εHf-units), which was digested once in Parr® bomb and once in DAS®, suggests inhomogeneity or somewhat incomplete digestion of an inherited zircon component (with lower εHf) in DAS® yielding a slightly higher $^{176}Hf/^{177}Hf$ by 0.000012 and (2) Andesite standard AGV-1 (Δ = 0.47 εHf-units), which was separated once by the three-stage separation scheme and once by single column separation.

Accuracy and reproducibility of $^{176}Lu/^{177}Hf$ by ID

Accuracy and reproducibility of $^{176}Lu/^{176}Hf$ by isotope dilution analysis (ID) in whole rock samples depends on (1) the precise knowl-

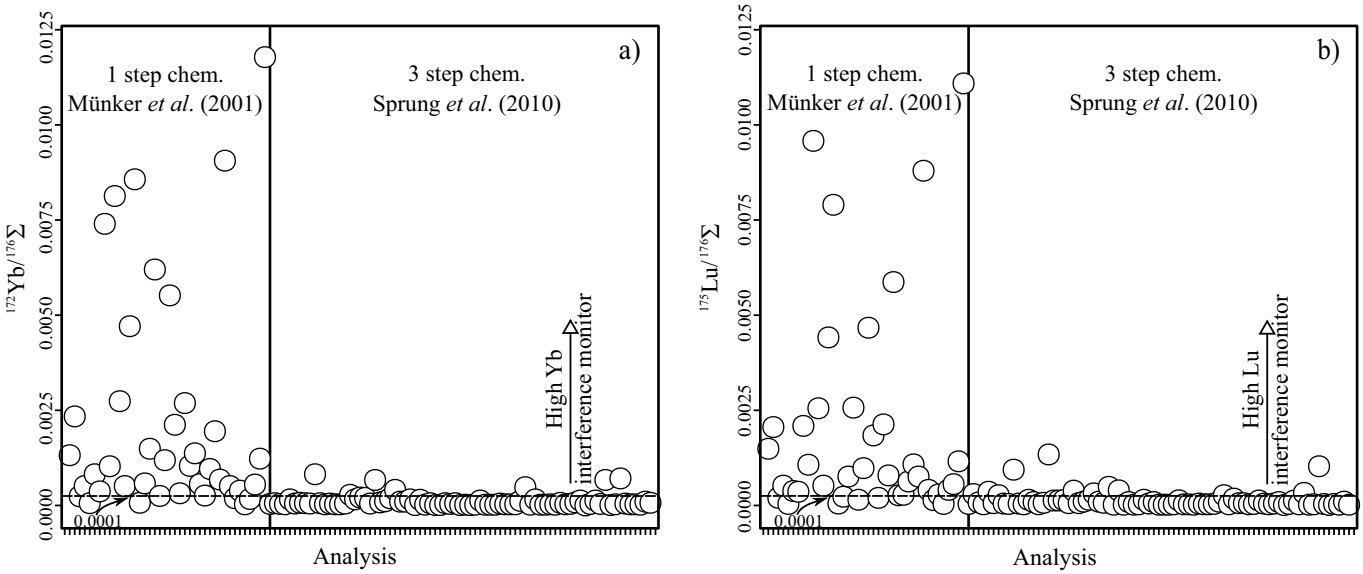

Figure 6. Interference monitors observed during Hf isotope analyses in our laboratory for different chemical separation methods (119 analysis from August 2012 to September 2015): (a) $^{172}Yb/^{176}\Sigma$ and (b) $^{175}Lu/^{176}\Sigma$. Note that $^{176}\Sigma=^{176}Yb+^{176}Lu+^{176}Hf$.

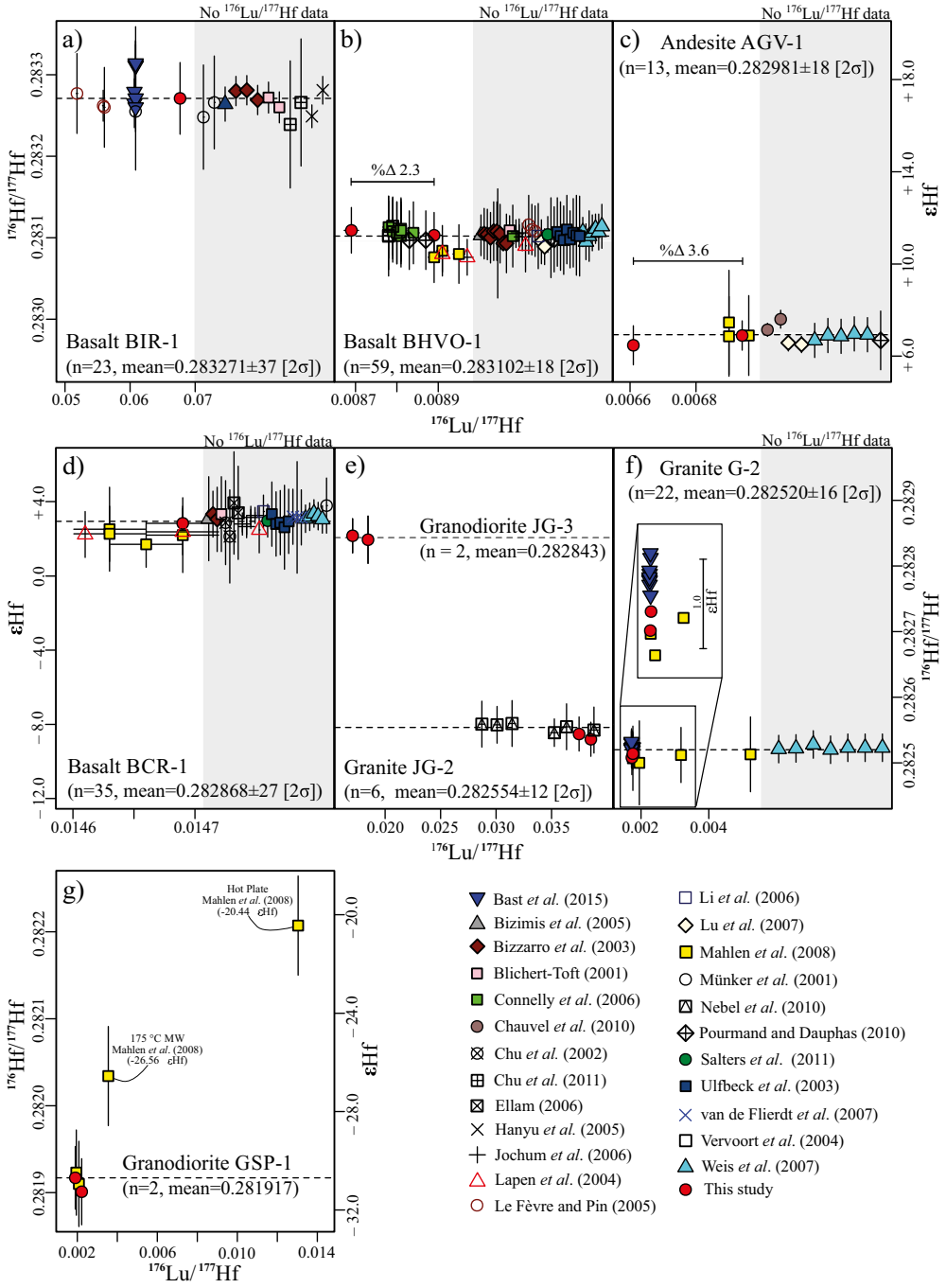

Figure 7. $^{176}Lu/^{177}Hf$ and $^{176}Hf/^{177}Hf$ data of (a) BIR-1, (b) BHVO-1, (c) AGV-1, (d) BCR-1, (e) JG-2 and JG-3, (f) G-2, and (g) GSP-1 international reference rock standards obtained in this study together with available data from literature (Table 1). Dashed lines represent the mean for compiled $^{176}Hf/^{177}Hf$ data, except for Granodiorite JG-3. The error bars are 2σ S.D.

edge of isotope compositions and concentrations of spike isotopes in the mixed spike, (2) equilibration between sample and spike, (3) adequate amount of spike for given Lu and Hf concentrations to avoid error amplification, and (4) in complete dissolution of all phases, in particular Hf-rich phases like zircon. Since all of these sources of error may worsen the overall accuracy and reproducibility and because not all laboratories do ID analyses, there are only few $^{176}Lu/^{177}Hf$ data published from the studied international reference rock standards to compare with. The published data are mostly from reference basalts (BCR, BHVO and BIR) and andesite AGV-1 (Münker *et al.*, 2001; Vervoort *et al.*, 2004; Lapen *et al.*, 2004; Le Fèvre and Pin, 2005; Connelly *et al.*, 2006; Mahlen *et al.*, 2008; Pourmand and Dauphas, 2010; Bast *et al.*, 2015). Only three publications present data from granitoid standards (Mahlen *et al.*, 2008; Nebel *et al.*, 2010; Bast *et al.*, 2015).

The best accuracy with respect to the reported $^{176}Lu/^{177}Hf$ values from mafic standards was obtained from basalt BCR-1 and from one analyses of andesite standard AGV-1, yielding deviations from the reported average values of 0.1% (Figure 7c and 7d). A second analysis of AGV-1 yielded a 3.8% lower $^{176}Lu/^{177}Hf$, mainly due to a 4% lower Lu-content, compared to the reference values (Figure 7c).

The $^{176}Lu/^{177}Hf$ from two analysis of BHVO-1 differ by 2.3% but the values are between -1.7 and 0.6% compared with the average of 20 reported values from literature (Table 5, Figure 7b). Basalt standard BIR-1 yielded a $^{176}Lu/^{177}Hf$ of 0.06659, which is 16.6% higher compared with the reported values (from 0.05184 to 0.06085, n = 11: Figure 7a). However, the Hf concentration calculated from our analysis is in agreement with the average value reported in literature (Table 5), suggesting that incomplete digestion was not an issue. Therefore, the difference is either due to poor sample-spike equilibration or inhomogeneity of BIR-1 with respect to Lu/Hf.

The $^{176}Lu/^{177}Hf$ values of granitic standard rocks differ from the most reliable reported values from 1.0 to 4.0% (G-2), -4.5 to 8.4% (GSP-1) and 12.1 to 15.3% (JG-2), respectively (Figure 7e–7g). Nevertheless, the large differences in the granite JG-2 and granodiorite GSP-1 may be due to the high dispersion of JG-2 data reported by Nebel *et al*. (2010) and the poorly reported GSP-1 data in literature (Figure 7e, 7g). The differences between duplicate analyses in granitoids standards vary from 2.3 (G-2) to 13.5% (GSP-1). It is noteworthy that for granitic whole-rock samples incomplete dissolution of refractory phases like zircon is the most problematic issue for $^{176}Lu/^{177}Hf$ reproducibility. Similar results were obtained for our replicate analyses from selected unknown samples. Whereas $^{176}Lu/^{177}Hf$ values from metabasite samples vary by acceptable 0.4 to 2.0%, Grenvillian orthogneisses differs by up to 43%, depending on the digestion method used (Table 5).

Although most $^{176}Hf/^{177}Hf$ and εHf values of the international reference rocks analyzed in this work agree, within analytical errors, with the data reported from literature, discrepancies in the $^{176}Lu/^{177}Hf$ values affect the recalculated initial $^{176}Hf/^{177}Hf_i$ and εHf_i values of ancient rock samples more severely. The effect on the initial values depends not only on the random and systematic errors introduced by instrumental counting statistics, mass-bias, and spike-stripping corrections, but also on the absolute $^{176}Lu/^{177}Hf$ and the error in age (which is not considered here). For example, a ±19.0% difference (between two replicate digestions) in the $^{176}Lu/^{177}Hf$ value of a Grenvillian orthogneiss (03-1b, $^{176}Lu/^{177}Hf$ = 0.00345 and 0.00426, Table 5) produces only ±0.43 εHf units difference in the initial value by recalculating to 1.0 Ga (Figure 8a). By assuming the same initial age and difference in $^{176}Lu/^{177}Hf$ for a metabasite (03-$2c_{(v2)}$, $^{176}Lu/^{177}Hf$ = 0.02454, Table 5) would change the εHf_{1Ga} by ±3.00 (Figure 8b). Hence, it is rather the absolute error of the $^{176}Lu/^{177}Hf$ values that counts for the time-integrated error in εHf_i and at a minor extent the percent error.

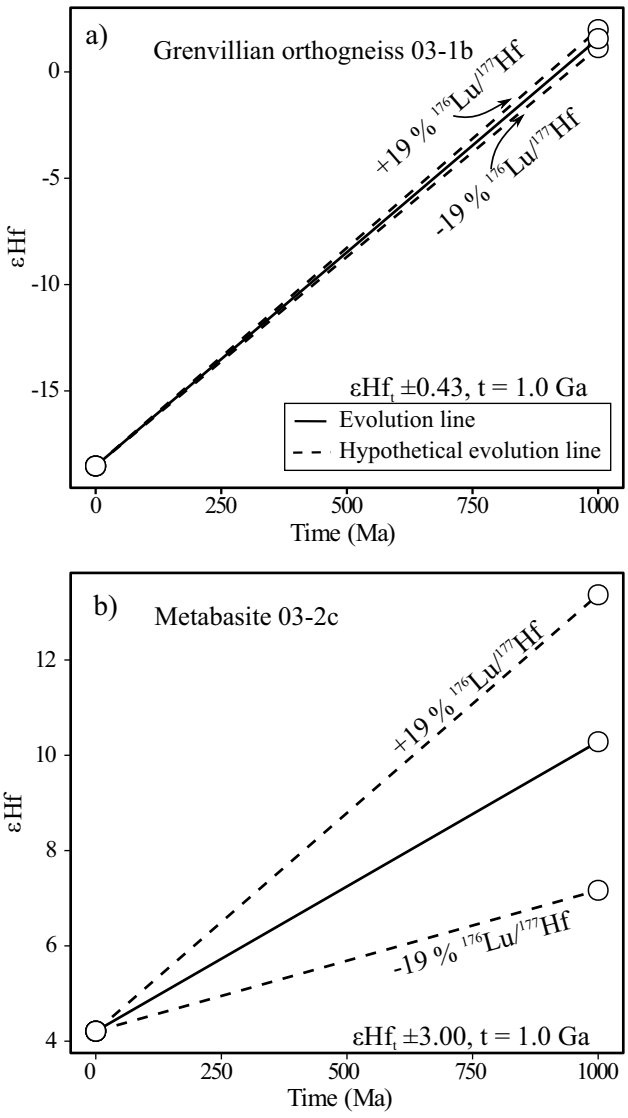

Figure 8. The εHf evolution diagram at 1.0 Ga (solid line) for (a) Grenvillian orthogneiss 03-1b (Parr® digested runs) and (b) metabasite 03-2c (v2). In addition, the hypothetical evolution lines (dashed lines) with a bias of ±19% in $^{176}Lu/^{177}Hf$ are shown.

Comparison of sample digestion techniques

Mahlen *et al*. (2008) tested the effects of four different digestion methods (tabletop hotplate, low-temperature microwave (175°C), high-temperature microwave (200°C), and Parr® bomb) for Lu-Hf isotope analysis of whole-rock samples. The authors concluded that any of the digestion methods might produce reliable $^{176}Hf/^{177}Hf$ values in mafic rocks. However, for felsic rocks incomplete digestion occurs with the tabletop hotplate and the low-temperature microwave methods that might affect not only $^{176}Lu/^{177}Hf$ but also the $^{176}Hf/^{177}Hf$ values.

In this work, the Picotrace DAS® digestion system is compared with the Parr® bomb digestion vessels. As mentioned above, there are only minor or insignificant differences in $^{176}Hf/^{177}Hf$ data between the two digestion system methods, but there are important differences in the $^{176}Lu/^{177}Hf$ values, particularly in some felsic rocks. Whereas lower $^{176}Lu/^{177}Hf$ values with the Picotrace DAS® digestion system compared with Parr® bomb digestion cannot be explained by incomplete dissolution but rather by poor sample-spike equilibration (mainly GSP-1 and JG-3), 19.0% and 43.3% higher $^{176}Lu/^{177}Hf$ values in orthogneiss samples performed with the Picotrace DAS® digestion system (03-1b and 03-2a) are most likely the result of incomplete dissolution of zircon. In such cases, assuming that complete sample-spike equilibration was achieved, the variations in $^{176}Lu/^{177}Hf$ and $^{176}Hf/^{177}Hf$ should correlate, and the data should plot along a regression line whose slope corresponds to the time of crystallization of the sample (Blichert-Toft *et al*., 2004; Lapen *et al*., 2004; Mahlen *et al*., 2008). If this is true – and the age of the rock is well-known – then incomplete dissolution of the whole-rock sample does not have any effect on the calculated initial $^{176}Hf/^{177}Hf$. On the other hand, if poor sample-spike equilibration or sample inhomogeneity is the case, then the data plot off the supposed reference isochron in a $^{176}Lu/^{177}Hf$ vs. $^{176}Hf/^{177}Hf$ plot. The different effects can be illustrated in $^{176}Lu/^{177}Hf$ vs. $^{176}Hf/^{177}Hf$ plots for samples with known age by including the corresponding reference isochrones (Figure 9).

The results from granitoids standards G-2 and GSP-1 (Figure 9a, 9b) are compared with the data published by Mahlen *et al.* (2008). The results from Parr® and DAS® digestion (this work) are similar to Parr® digestion by Mahlen *et al.* (2008). Slightly differing results, however, do not plot on the reference isochrones, indicating sample inhomogeneity and/or poor equilibration with spike instead of incomplete dissolu-

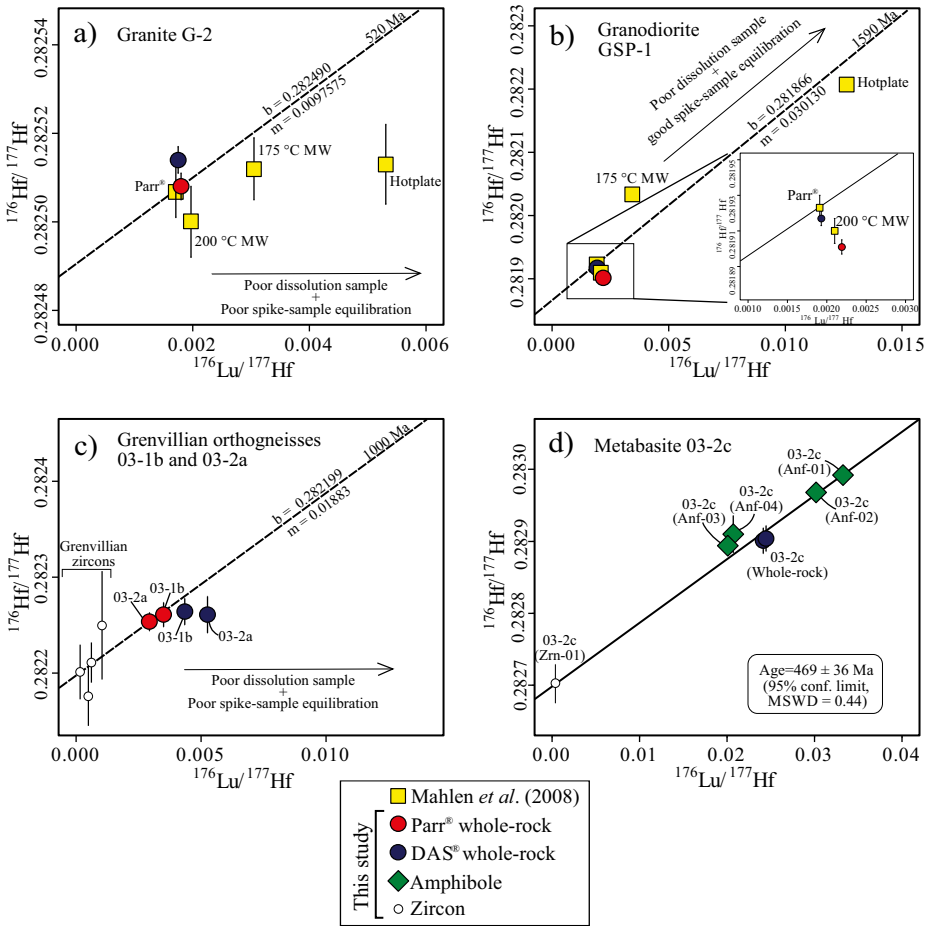

Figure 9. $^{176}Lu/^{177}Hf$ *vs.* $^{176}Hf/^{177}Hf$ isochron diagrams for (a,b) zircon-bearing international reference rocks standards (G-2 and GSP-1), (c) orthogneiss samples (03-1b and 03-2a), and (d) metabasite sample (03-2c). Reference isochrons of the standard granitoids correspond to their reported ages, which were plotted through the average from data points of Parr® bomb digestion. The slope of the reference isochron for orthogneiss samples corresponds to their 1.0 Ga U-Pb zircon age reported by González-Guzmán *et al.* (2014) and is plotted through the zircon data point. Discrepancies introduced by incomplete sample dissolution or incomplete spike-sample equilibration are illustrated by the deviations from the calculated reference isochrones. Note that the largest deviations are associated with samples processed using tabletop hotplate dissolution (~120 °C, Mahlen *et al.*, 2008). The five-point isochron for the amphibolite 03-2c (d) is calculated from two whole rock aliquots, two magnetic hornblende (Anf-01 and Anf-02) separates, and one zircon. Note that secondary low-magnetic amphiboles (Anf-03 and Anf-04) plot off the isochrones, indicating later-stage alteration (error bars are 1σ S.D.)

tion, as observed in the hot plate digestion and the low-temperature microwave methods (Figure 9a, 9b; Mahlen *et al.*, 2008). On the other hand, replicate analyses of garnet-bearing sample R0907 show a slight but significant difference in the $^{176}Lu/^{177}Hf$ value (4.4 %). However, this discrepancy is most likely the result of sample inhomogeneity and not incomplete sample digestions, since higher Lu and Hf concentrations were obtained by DAS® (Table 5).

Inasmuch as zircon has high Hf and low Lu concentrations typically of about 1% Hf and Lu in the 100 ppm-range, measured Hf isotope ratios of zircon are close to their initial values and therefore insensitive to uncertainties in $^{176}Lu/^{177}Hf$. On a $^{176}Lu/^{177}Hf$ *vs.* $^{176}Hf/^{177}Hf$ plot (Figure 9c) the results of whole-rock analysis from Grenvillian orthogneisses (samples 03-1b and 03-2a) digested with Parr® together with the results from four Parr® digested zircon grains, plot within errors on a 1.0 Ga reference isochron that corresponds to the approximate U-Pb zircon age of the rocks (Manjarrez-Juárez, 2013; González-Guzmán *et al.*, 2014). The data from the same whole-rock samples digested with DAS® do not plot on this reference isochron (Figure 9c). The offset of DAS® digested runs suggests incomplete sample dissolution. The observed differences between DAS® and Parr® bomb digestion is due to large differences in the Hf concentrations determined by ID between DAS® digestion (17.5 and 14.8 ppm Hf) and Parr® bomb digestion that yielded 25.6 and 28.7 ppm Hf, for sample 03-1b and sample 03-2a, respectively. Hence, samples with relatively high Hf contents that implies also high zircon content are most vulnerable to incomplete digestion if temperatures are below 190°C typically used in Parr® bombs.

For the relatively zircon-poor metabasite samples, incomplete sample digestion is not observed and whole-rock analyses are reproducible by using DAS® with differences in $^{176}Lu/^{177}Hf$ of 2.0% or less and $\Delta\varepsilon Hf_t$ between replicate analysis at 450 Ma (regional high-grade event, González-Guzmán *et al.*, 2014) of 0.11 (sample 03-2b), 0.17 (sample 03-2c) and 0.07 (sample 05-1a) εHf-units. From the sample 03-2c, in addition to duplicate analysis of the whole-rock powder, a single zircon grain (Parr® bomb digestion) and four amphibole concentrates (two primary and two secondary) were performed with DAS® digestion (Table 5). The primary amphiboles (Anf-01 and Anf-02), yielding $^{176}Lu/^{177}Hf$ greater than the whole-rock, plot on a regression line together with the whole-rock and zircon in a $^{176}Lu/^{177}Hf$ *vs.* $^{176}Hf/^{177}Hf$ diagram (Figure 9d). The slope of this regression line corresponds to an age of 469 ± 36 Ma (95% conf. limit, MSWD = 0.44), which is within errors identi-

cal to the time of high-grade metamorphism and anatexis in the area (González-Guzmán *et al*., 2014). The secondary amphiboles (Anf-03 and Anf-04) with $^{176}Lu/^{177}Hf$ lower than whole-rock, plot above the isochron confirming their secondary origin. The results demonstrate that besides complete sample dissolution with DAS® digestion, both spike-sample equilibration and accurate spike-subtraction was attained.

CONCLUSIONS AND RECOMMENDATIONS

The three-stage chemical separation technique of Lu and Hf from whole-rock samples applied in this study (modified from Sprung *et al*., 2010) yielded significantly better results compared to the single-stage separation technique after Münker *et al*. (2001), with virtually no isobaric interferences of ^{176}Lu and ^{176}Yb on the ^{176}Hf signal. The $^{176}Hf/^{177}Hf$ values calculated with IsotopeHf® data reduction that includes spike and mass bias corrections yields reliable results. Accuracy and reproducibility of $^{176}Lu/^{177}Hf$ by ID depend on the digestion method, sample-spike equilibrium, and homogeneity of the sample aliquot. Sample digestion with the Picotrace DAS® pressure digestion system at 165°C is reproducible and comparable with digestion in Parr® bombs at 190°C for mafic rocks and felsic rocks with moderate Hf content (<15 ppm). For Hf-rich rocks that incorporate most of their Hf in zircon complete sample dissolution cannot be achieved with the DAS® at 165°C, producing large errors on $^{176}Lu/^{177}Hf$ values and consequently erroneous initial Hf isotope ratios for ancient rock samples. For zircon-rich whole-rock samples the Parr® bomb digestion method at 190°C for five days is recommended or the DAS® pressure digestion system should be improved by reducing temperature loss to achieve significantly higher internal temperature.

ACKNOWLEDGEMENTS

This contribution was supported by Consejo Nacional de Ciencia y Tecnología (CONACyT, Convocatoria Ciencia Básica 2012, project 180588). The authors wish to thank Juan Pablo Bernal-Uruchurtu, Juliana Estrada-Carmona, Carlos Ortega-Obregón, and Ofelia Pérez-Arvizu for their help with data acquisition at Centro de Geociencias-Universidad Nacional Autónoma de México. Thanks go also to Mariela Carrera-Muñoz and Sergio Padilla-Ramírez (Centro de Investigación Científica y de Educación Superior de Ensenada) for running the clean lab and sample preparation. Special thanks go to Erik Scherer (Universität Münster), for donating us some Lu-Hf spike and for his advices in improving the Lu-Hf methodology in this work. We thank to Mauricio Ibanez-Mejia (Massachusetts Institute of Tecnology) and Uwe Martens (Tectonic Analysis Inc.) for their careful reviews of the manuscript and their insightful comments and suggestions. Finally, we thank Peter Schaaf for his editorial handling.

REFERENCES

Ando, A., Shibata, K., 1988, Isotope data and rare gas composiuons of GSJ rock reference samples, "Igneous rock series": Geochemical Journal, 22, 149-156.

Barfod, G.H., Otero, O., Albarède, F., 2003, Phosphate Lu-Hf geochronology: Chemical Geology, 200 (3-4), 241-253.

Bast, R., Scherer, E.E., Sprung, P., Fischer-Gödde, M., Stracke, A., Mezger, K., 2015, A rapid and efficient ion-exchange chromatography for Lu–Hf, Sm–Nd, and Rb–Sr geochronology and the routine isotope analysis of sub-ng amounts of Hf by MC-ICP-MS: Journal of Analytical Atomic Spectrometry, 30, 2323-2333.

Bayon, G., Burton, K.W., Soulet, G., Vigier, N., Dennielou, B., Etoubleau, J., Ponzevera, E., 2009, Hf and Nd isotopes in marine sediments: constraints on global silicate weathering: Earth and Planetary Science Letter, 277, 318-326.

Bizimis, M., Sen, G., Salters, V.J.M., Keshav, S., 2005, Hf-Nd-Sr isotope systematics of garnet pyroxenites from Salt Lake Crater, Oahu, Hawaii: Evidence for a depleted component in Hawaiian volcanism: Geochimica et Cosmochimica Acta, 69 (10), 2629-2646.

Bizzarro, M., Baker, J.A., Ulfbeck, D., 2003, A new digestion and chemical separation technique for rapid and highly reproducible determination of Lu/Hf and Hf isotope ratios in geological materials by MC-ICP-MS: Geostandards Newsletter, 27 (2), 133-145.

Blichert-Toft, J., 2001, On the Lu-Hf isotope geochemistry of silicate rocks: Geostandards Newsletter 2001, 25 (1), 41-56.

Blichert-Toft, J., Puchtel, S., 2010, Depleted mantle sources through time: Evidence from Lu–Hf and Sm–Nd isotope systematics of Archean komatiites: Earth and Planetary Science Letters, 297, 598-606.

Blichert-Toft, J., Chauvel, C., Albarède, F., 1997, Separation of Hf and Lu for high-precision isotope analysis of rock samples by magnetic sector-multiple collector ICP-MS: Contributions to Mineralogy and Petrology, 127 (3), 248-260.

Blichert-Toft, J., Arndt, N.T., Gruau, G., 2004, Hf isotopic measurements on Barberton komatiites: effects of incomplete sample dissolution and importance for primary and secondary magmatic signatures: Chemical Geology, 207 (3), 261-275.

Boelrijk, N., 1968, A general formula for "double" isotope dilution analysis: Chemical Geology, 3 (4), 323-325.

Bouvier, A., Vervoort, J.D., Patchett, P.J., 2008, The Lu–Hf and Sm–Nd isotopic composition of CHUR: Constraints from unequilibrated chondrites and implications for the bulk composition of terrestrial planets: Earth and Planetary Science Letters, 273 (1-2), 48-57.

Cai, Y., LaGatta, A., Goldstein, S., Langmuir, C., Gómez-Tuena, A., Martín-del Pozzo, A.L., Carrasco-Núñez, G., 2014, Hafnium isotope evidence for slab melt contributions in the Central Mexican Volcanic Belt and implications for slab melting in hot and cold slab arcs: Chemical Geology, 377, 44-55.

Chauvel, C., Bureau, S., Poggi, C., 2010, Comprehensive chemical and isotopic analyses of basalt and sediment reference materials: Geostandards and Geoanalytical Research, 35 (1), 125-143.

Chu, N.C., Taylor, R.N., Chavagnac, V., Nesbitt, R.W., Boella, R.M., Milton, J.A., German, C.R., Bayon, G., Burton, K., 2002, Hf isotope ratio analysis using Multi-Collector Inductively Coupled Plasma Mass Spectrometry: an evaluation of isobaric interference corrections: Journal of Analytical Atomic Spectrometry, 17 (12), 1567-1574.

Chu, Z.Y., Yang, Y.H., Jinghui, G., Qiao, G.S., 2011, Calculation methods for direct internal mass fractionation correction of spiked isotopic ratios from Multi-collector mass spectrometric measurements: International Journal of Mass Spectrometry, 299 (2), 87-93.

Connelly, J.N., Ulfbeck, D.G., Thrane, K., Bizzarro, M., Housh, T., 2006, A method for purifying Lu and Hf for analyses by MC-ICP-MS using todga resin: Chemical Geology, 233 (1), 126-136.

Ellam, R.M., 2006, New constraints on the petrogenesis of the Nuanetsi picrite basalts from Pb and Hf isotope data: Earth and Planetary Science Letters, 245 (1-2), 153-161.

Estrada-Carmona, J., Weber, B., Scherer, E.E., Martens U., Elías-Herrera, M., 2016, Lu-Hf geochronology of Mississippian high-pressure metamorphism in the Acatlán Complex, southern México: Gondwana Research, 34, 174-186.

Flanagan, F.J., 1967, U.S. Geological Survey silicate rock standards: Geochimica at Cosmochimica Acta, 31, 289-308.

Flanagan, F.J., 1984, Three USGS mafic rock reference samples, W-2, DNC-1, and BIR-1, U.S.: Geological Survey Bulletin 1623, 54 pp.

González-Guzmán, R., Weber, B., Manjarrez-Juárez, R., Hecht, L., Solari, L., 2014, Petrogenesis of basement rocks in the southern Chiapas Massif: Implications on the tectonic evolution of the Maya Block [abstract]: Mineralogical Magazine, 839.

Gopalan, K., 2002, Direct correction for mass fractionation of spiked isotopic ratios from dynamic multicollector measurements: Geochemical Journal, 36 (1), 83-89.

Gramlich, J.W., Murphy, T.J., Garner, E.L., Shields, W.R., 1973, Absolute isotopic abundance ratio and atomic weight of a reference sample of rhenium:

Journal of Research of the *National Bureau* of Standards, Section A: *Physics* and *Chemistry*, 77A, 691.

Guitreau, M., Blichert-Toft, J., Mojzsis, S.J., Roth, A.S.G., Bourdon, B., 2013, A legacy of Hadean silicate differentiation inferred from Hf isotopes in Eoarchean rocks of the Nuvvuagittuq supracrustal belt (Québec, Canada): Earth and Planetary Science Letters, 362, 171-181.

Guo, P., Niu, Y., Sun, P., Ye, L., Liu, J., Zhang, J., Feng, Y., Zhao, J., 2016, The origin of Cenozoic basalts from central Inner Mongolia, East China: The consequence of recent mantle metasomatism genetically associated with seismically observed paleo-Pacific slab in the mantle transition zone: Lithos, 240–243, 104–118.

Hanyu, T., Nakai, S., Tatsuta, R., 2005, Hafnium isotope ratios of nine GSJ reference samples: Geochemical Journal, 39 (1), 83-90.

Jochum, K.P., Stoll, B., Herwig, K., Willbold, M., Hofmann, A.W., Amini, M., Aarburg, S., Abouchami, W., Hellebrand, E., Mocek, B., Raczek, I., Stracke, A., Alard, O., Bouman, C., Becker, S., Ducking, M., Bratz, H., Klemd, R., de Bruin, D., Canil, D., Cornell, D., de Hoog, C.J., Dalpe, C., Danyushevsky, L., Eisenhauer, A., Gao, Y.J., Snow, J.E., Goschopf, N., Gunther, D., Latkoczy, C., Guillong, M., Hauri, E.H., Hofer, H.E., Lahaye, Y., Horz, K., Jacob, D. E., Kassemann, S.A., Kent, A.J.R., Ludwig, T., Zack, T., Mason, P.R.D., Meixner, A., Rosner, M., Misawa, K.J., Nash, B.P., Pfander, J., Premo, W.R., Sun, W.D., Tiepolo, M., Vannucci, R., Vennemann, T., Wayne, D., Woodhead, J.D., 2006, Mpi-ding reference glasses for in situ microanalysis: New reference values for element concentrations and isotope ratios: Geochemistry, Geophysics, Geosystems, 7 (2), 1-44.

Kleinhanns, I.C., Kreissig, K, Nägler, T.F., Kamber, B.S., Meisel, T., Kramers, J.D., 2002 Combined chemical separation of Lu, Hf, Sm, Nd, and REEs from a single rock digest: Precise and accurate isotope determination of Lu-Hf and Sm-Nd using multicollector-ICPMS: Analytical Chemistry, 74 (1), 67-73.

Lapen, T.J., Mahlen, N.J., Johnson, C.M., Beard, B.L., 2004, High precision Lu and Hf isotope analyses of both spiked and unspiked samples: a new approach: Geochemistry, Geophysics, Geosystems, 5 (1), 1-17.ne

Larsson, D., Söderlund, U., 2005, Lu–Hf apatite geochronology of mafic cumulates: An example from a Fe–Ti mineralization at Smålands Taberg, southern Sweden: Chemical Geology, 224, 201-211.

Le Fèvre, B., Pin, C., 2001, An extraction chromatography method for Hf separation prior to isotopic analysis using multiple collection ICP-mass spectrometry: Analytical Chemistry, 73 (11), 2453-2460.

Le Fèvre, B., Pin, C., 2005, A straightforward separation scheme for concomitant Lu-Hf and Sm-Nd isotope ratio and isotope dilution analysis: Analytica Chimica Acta, 543 (1), 209-221.

Li, X.-H., Li, Z.-X., Wingate, M.T.D, Chung, S.-L., Liu, Y., Lin, G.-C., Li, W.-X., 2006, Geochemistry of the 755 Ma Mundine Well dyke swarm, northwestern Australia: Part of a Neoproterozoic mantle superplume beneath Rodinia?: Precambrian Research, 146, 1-15.

Lu, Y., Makishima, A., Nakamura, E., 2007, Purification of Hf in silicate materials using extraction chromatographic resin, and its application to precise determination of $^{176}Hf/^{177}Hf$ by MC-ICP-MS with ^{179}Hf spike: Journal of Analytical Atomic Spectrometry, 22 (1), 69-76.

Mahlen, N.J., Beard, B.L., Johnson, C.M., Lapen, T.J., 2008, An investigation of dissolution methods for Lu-Hf and Sm-Nd isotope studies in zircon- and garnet-bearing whole-rock samples: Geochemistry, Geophysics, Geosystems, 9 (1), 1-16.

Manjarrez-Juárez, R.U., 2013, Basamento grenviliano y orogénesis ordovícica en el sur del Macizo de Chiapas: Implicaciones paleogeográficas para el Bloque Maya Sur en el Paleozoico temprano: Master thesis, Centro de Investigación Científica y de Educación Superior de Ensenada, Baja California, 115 pp.

Maréchal, C.N., Télouk, P., Albarède, F., 1999, Precise analysis of copper and zinc isotopic compositions by plasma-source mass spectrometry: Chemical Geology, 156 (1), 251-273.

Münker, C., Weyer, S., Scherer, E., Mezger, K., 2001, Separation of high field strength elements (Nb, Ta, Zr, Hf) and Lu from rock samples for MC-ICP-MS measurements: Geochemistry, Geophysics, Geosystems, 2, 1-19.

Nebel, O., Mezger, K., Scherer, E., Münker, C., 2005, High precision determinations of $^{87}Rb/^{85}Rb$ in geologic materials by MC-ICP-MS: International Journal of Mass Spectrometry: 246 (1), 10-18.

Nebel, O, Vroon, P, Wiggers de Vries, D., Jenner, F.E., Mavrogenes, J.A., 2010, Tungsten isotopes as tracers of core-mantle interactions: The influence of subducted sediments: Geochimica et Cosmochimica Acta, 74, 751-762.

Nebel-Jacobsen, J., Scherer, E.E., Münker, C., Mezger, K., 2005, Separation of U, Pb, Lu, and Hf from single zircons for combined U–Pb dating and Hf isotope measurements by TIMS and MC-ICPMS: Chemical Geology, 220, 105-120.

Patchett, P., Tatsumoto, M., 1980, A routine high-precision method for Lu-Hf isotope geochemistry and chronology: Contributions to Mineralogy and Petrology, 75 (3), 263-267.

Pourmand, A., Dauphas, N., 2010, Distribution coefficients of 60 elements on TODGA resin: Application to Ca, Lu, Hf, U and Th isotope geochemistry: Talanta, 81, 741-753.

Qiao, G., 1988, Normalization of isotopic dilution analysis – a new program for Isotope Mass Spectrometric analysis: Science China Mathematics, 31 (10), 1236-1268.

R Core Team, 2016, R: A language and environment for statistical computing: Vienna, Austria, R Foundation for Statistical Computing, <https://www.R-project.org/>.

Russell, W., Papanastassiou, D., Tombrello, T., 1978, Ca isotope fractionation on the Earth and other solar system materials: Geochimica et Cosmochimica Acta, 42 (8), 1075-1090.

Salters, V.J.M., Mallick, S., Hart, S.R., Langmuir, C.E., Stracke, A., 2011, Domains of depleted mantle: new evidence from Hafnium and Neodymium isotopes: Geochemistry Geophysics Geosystems, 12 (8).

Scherer, E., Münker, C., Rehkämper, M., Mezger, K., 1999, Improved precision of Lu isotope dilution measurements by MC-ICP-MS and application to Lu-Hf geochronology [abstract]: Eos, 80 (46), p. 1118.

Scherer, E., Münker, C., Mezger, K., 2001, Calibration of the Lutetium-Hafnium clock: Science, 293 (5530), 683-687.

Schmitz, M., Vervoort, J., Bowring, S., Patchett, P., 2004, Decoupling of the Lu-Hf and Sm-Nd isotope systems during the evolution of granulitic lower crust beneath southern Africa: Geology, 32(5), 405-408.

Segal, I., Halicz, L., Platzner, I.T., 2003, Accurate isotope ratio measurements of ytterbium by multiple collection inductively coupled plasma mass spectrometry applying erbium and hafnium in an improved double external normalization procedure: Journal of Analytical Atomic Spectrometry 18(10), 1217-1223.

Skora, S., Baumgartner, L.P., Mahlen, N.J., Johnson, C.M., Pilet, S., Hellebrand, E., 2006, Diffusion-limited REE uptake by eclogite garnets and its consequences for Lu–Hf and Sm–Nd geochronology: Contributions to Mineralogy and Petrology 152 (6), 703-720.

Smit, M.A., Scherer, E.E., Brocker, M., van Roermund, H.L.M., 2010, Timing of eclogite facies metamorphism in the southernmost Scandinavian Caledonides by Lu-Hf and Sm-Nd geochronology: Contributions to Mineralogy and Petrology 159 (4), 521-539.

Söderlund, U., Patchett, J.P., Vervoort, J.D., Isachsen, C., 2004, The ^{176}Lu decay constant determined by Lu–Hf and U–Pb isotope systematics of Precambrian mafic intrusions: Earth and Planetary Science Letters 219, 311-324.

Sprung, P., Scherer, E., Upadhyay, D., Leya, I., Mezger, K., 2010, Non-nucleosynthetic heterogeneity in non-radiogenic stable Hf isotopes: Implications for early solar system chronology: Earth and Planetary Science Letters, 295 (1), 1-11.

Ulfbeck, D., Baker, J., Waight, T., Krogstad, E., 2003, Rapid sample digestion by fusion and chemical separation of Hf for isotopic analysis by MC-ICPMS: Talanta, 59 (2), 365-373.

van de Flierdt, T., Goldstein, S.L., Hemming, S.R., Roy, M., Frank, M., Halliday, A.N., 2007, Global Neodymium-Hafnium isotope systematics—revisited: Earth and Planetary Science Letters, 259 (3), 432-441.

Vervoort, J.D., Patchett, P.J., Blichert-Toft, J., Albarède, F., Downes, H., Rudnick, R., 2000, Hf-Nd isotopic evolution of the lower crust: Earth and Planetary Science Letters, 181, 115-129.

Vervoort, J.D., Patchett, P.J., Söderlund, U., Baker, M., 2004, Isotopic composition of Yb and the determination of Lu concentrations and Lu/Hf ratios by isotope dilution using MC-ICPMS: Geochemistry, Geophysics, Geoystems, 5 (11), 1-15.

Vervoort, J.D., Plank, T., Prytulak, J., 2011, The Hf-Nd isotopic composition of marine sediments: Geochimica at Cosmochim Acta, 75, 5903-5926.

Weber, B., Valencia, V.A., Schaaf, P., Pompa-Mera, V., Ruiz, J., 2008, Significance of Provenance Ages from the Chiapas Massif Complex (Southeastern

Mexico): Redefining the Paleozoic Basement of the Maya Block and Its Evolution in a Peri-Gondwanan Realm: Journal of Geology, 116, 619-39.

Weber, B., Scherer, E., Valencia, V.A., Schulze, C.H., Montecinos-Muñoz, P.R., Mezger, K., Ruiz, J., 2010, U-Pb and Lu-Hf Isotope systematics of lower crust from central-southern Mexico- geodynamic significance of Oaxaquia in a Rodinia realm: Precambrian Research, 182(1-2), 149-162.

Weis, D., Kieffer, B., Hanano, D., Nobre-Silva, I., Barling, J., Pretorius, W., Maerschalk, C., Mattielli, N., 2007, Hf isotope compositions of US Geological Survey reference materials: Geochemistry, Geophysics, Geosystems, 8 (6), 1-15.

Wickham, H., 2009, ggplot2: Elegant Graphics for Data Analysis, New York, Springer-Verlag 211 pp. <https://CRAN.R-project.org/package=ggplot2>

Wickham, H., 2011, The Split-Apply-Combine Strategy for Data Analysis: Journal of Statistical Software, 40(1), 1-29. https://CRAN.R-project.org/package=plyr.

Wickham, H., Francois, R., 2015, dplyr: A Grammar of Data Manipulation. R package version 0.4.3 <https://CRAN.R-project.org/package=dplyr >.

Wieser, M.E., Holden, N., Coplen, T.B., Böhlke, J.K., Berglund, M., Brand, W.A., De Bièvre, P., Gröning, M., Loss, R.D., Meija, J., Hirata, T., Prohaska, T., Schoenberg, R., O'Connor, G., Walczyk, T., Yoneda, S., Zhu, X.K., 2013, Atomic Weights of the Elements 2011: Pure and Applied Chemistry, 85, 1047-1078.

Wimpenny, J.B., Amelin, Y., Yin, Q.Z., 2013, Precise determination of the lutetium isotopic composition in rocks and minerals using multicollector ICPMS: Analytical Chemistry, 85 (23), 11258-11264.

Yang, Y.H., Zhang, H.F., Chu, Z.Y., Xie, L.W., Wu, F., 2010, Combined chemical separation of Lu, Hf, Rb, Sr, Sm and Nd from a single rock digest and precise and accurate isotope determinations of Lu–Hf, Rb–Sr and Sm–Nd isotope systems using Multi-Collector ICP-MS and TIMS: International Journal of Mass Spectrometry, 290 (2), 120-126.

Manuscript received: February 7, 2016
Corrected manuscript received: June 3, 2016
Manuscript accepted: June 16, 2016